CHEMICAL REVIEWS

REVIEW

pubs.acs.org/CR

Computational Prediction of ^{1}H and ^{13}C Chemical Shifts: A Useful Tool for Natural Product, Mechanistic, and Synthetic Organic Chemistry

Michael W. Lodewyk,[†,§] Matthew R. Siebert,[‡,§] and Dean J. Tantillo*[,†]

[†]Department of Chemistry, University of California—Davis, Davis, California 95616, United States

[‡]Department of Chemistry and Biochemistry, Texas Tech University, Lubbock, Texas 79409, United States

Supporting Information

CONTENTS

1. INTRODUCTION

Quantum mechanical calculations of magnetic behavior in molecules are present in the literature dating at least as far back as London's treatment of diamagnetic anisotropy in aromatic compounds in 1937.[1] In the early 1950s, Ramsey published a series of eight papers delineating equations used to calculate NMR chemical shift and spin−spin coupling constants.[2] By 1963, Hameka's thorough account on the state of quantum chemistry at the time described equations for magnetic susceptibilities and other quantities related to magnetic resonance, as well as numerous other molecular properties.[3] However, routine determination of isotropic shielding constants (and thus chemical shifts) was not practical until the advent of methods focused on overcoming the "gauge problem".[4] Most notable among these are the gauge-including atomic orbital (GIAO)[5] and individual gauges for localized orbitals (IGLO)[6,7] methods. Although GIAO techniques have a longer history in the literature, it was Kutzelnigg's IGLO methods that first led to practical applications of computed shielding constants and chemical shifts, beginning with the 1987 seminal work of Schindler in carbocation structure elucidation.[8] Although the methods here were not successful in every case considered, the initial shortcomings (later found to be mainly related to accurate molecular geometries) were quickly overcome, and the field was vigorously developed by Schleyer

Received: April 7, 2011
Published: November 17, 2011

and co-workers, with notable contributions from other authors as well.[9−14] Here, Schleyer coined the terms "ab initio/IGLO" and "GIAO/NMR" to describe the use of IGLO, and later GIAO, techniques for structure elucidation. These approaches paved the way for the broad use of computed chemical shifts for structure elucidation in organic molecules, which is a major focus of this review. Advances in this area have continued up through today with several notable contributions from Rasul, Olah, and co-workers.[15] Finally, it should be noted that the original formulation of GIAO was further refined by Pulay and co-workers,[16,17] a development that subsequently led to its incorporation into popular commercial software packages. GIAO is now the method of choice for most NMR calculations. Additional information and details related to the history of NMR calculations can be found in several excellent books, reviews, and other accounts.[9,10,13,14,18,19]

Over the past decade, computational modeling of ^{1}H and ^{13}C chemical shifts has seen a marked increase in accuracy, affordability, and application. These improvements come from many sources, including advancements in both computational techniques and in computers themselves; the result is that reliable chemical shift calculations are now routinely accessible to organic chemists. This tutorial review aims (1) to increase awareness of theoretical approaches to computing chemical shifts, (2) to facilitate the effective application of these techniques to common problems encountered in organic chemistry, and (3) to serve as a practical guide to organic chemists who wish to augment their research with computed chemical shifts. We will not attempt to provide an in-depth discussion of the theoretical foundations of the field of computational NMR, since numerous excellent articles in these areas already exist. For example, the reader is directed to the 2004 book edited by Kaupp, Bühl, and Malkin[14] (see in particular Table 2.1) as well as the 2008 Casabianca and de Dios review along with the extensive annotated list of earlier reviews contained therein.[20] Other reviews include those by Mulder et al.,[21] Alonso-Gómez et al.,[22] Siehl,[10] Barone et al.,[23] Bifulco et al.,[24] Bagno et al.,[25] and Jaszuński et al.[26] Further, the vast volume of literature concerned with these areas prevents us from presenting an exhaustive review; rather, we will present key background information, examples, and more recent techniques. Readers interested in computing proton−proton coupling constant data are directed to the work of Bally and Rablen for practical considerations and leading references.[27]

In the remainder of section 1 we will survey applications of computed NMR shifts; this will provide a sense for the many problems an organic chemist may encounter to which these techniques may be applied. We will close section 1 with a discussion of the basic steps involved in NMR chemical shift calculations. Section 2 outlines the major sources of error in NMR calculations, and section 3 discusses techniques that may be used to overcome them. In section 4, we compare and contrast the specific methods that are available today for running NMR calculations. In section 5, we recommend for methods for computation of chemical shift data. After some concluding remarks in section 6, we present a brief Appendix, in which we discuss our repository of linear regression scaling factors for ^{1}H and ^{13}C nuclei, available at http://cheshireNMR.info.

1.1. Applications

The reasons why an organic chemist may want to pursue NMR calculations are as varied as those for taking experimental NMR spectra themselves. One of the most basic applications of NMR calculations is to assist in assigning spectra. Experimental NMR spectra typically provide a thorough description of the hydrocarbon framework of organic molecules, but a complete one-to-one assignment of observed shifts to individual nuclei is often very challenging, even with advanced multidimensional NMR techniques (vide infra).[22,28−35] Here computed NMR chemical shifts provide a distinct advantage, since there is always a clear one-to-one correspondence between the computed chemical shifts and the nuclei that give rise to them. Traditionally, researchers often look to the common increment techniques available in software packages such as ChemOffice,[36] MestReNova,[37] and ACD,[38] which are simple to use and often provide satisfactory results for "normal" organic molecules (molecules containing functional groups and geometric features that do not stray far from those used in deriving the increment values themselves and molecules which lack through-space intramolecular interactions and stereoelectronic features that are not included in the increment values). However, modern quantum mechanical techniques prove to be significantly more accurate and reliable than the increment methods and are much more capable of treating unusual systems (see section 4.3.1).[39]

A representative example of the use of quantum chemical techniques to reassign a complex spectrum is found in a 1998 report by Facelli.[40] Here, computed chemical shifts were used to revise the assignment of peaks observed for methyl bacteriopheophorbide *a* and methyl bacteriochlorophyll *a*; the data for the former is shown in Figure 1. Many other examples of using chemical shift calculations to assign or reassign experimental spectra have been reported as well.[4,41−48]

In addition to the analysis of experimental spectra for known (or strongly suspected) structures, perhaps the broadest category of computed NMR applications is the elucidation of chemical structures. Despite the wealth of information provided by one- and two-dimensional experimental NMR techniques, these spectra alone often do not provide unambiguous proof of the precise stereochemical features or sometimes even the basic connectivity of complicated molecules, since significant differences in structure can sometimes lead to only subtle differences in their spectra. NMR calculations of sufficient quality to distinguish between closely related structures are now readily attainable.[24,31,49−54] For example, Figure 2 shows the natural product vannusal B, the structure of which was originally proposed and subsequently revised to a different diastereomer on the basis of experimental NMR data.[49] After the structure was revised, Bagno and co-workers examined the computed ^{1}H and ^{13}C chemical shifts of all diastereomers synthesized along the way to the final revision.[49] Their results demonstrate that the computed data could have identified the most likely diastereomers and ruled out several for which the data is a poor match. In fact, the computed NMR data for the correct structure was the closest match to the experimental data out of all the structures examined for this natural product. For an example of the use of chemical shift calculations helping to determine the correct diastereomer of a natural product before it was synthesized, see the recent case of nobilisitine A.[55,56]

Of particular note here is the recent development of advanced statistical analyses (CP3 and DP4) for assigning relative configurations based solely on computed chemical shifts; these analyses are readily employed in part due to the availability of a Web-based applet provided by Smith and Goodman[50−52] and have been successfully applied in our own work.[55] One noteworthy example of the utility of the DP4 analysis is the case of Ardisson's polyketide (Figure 3).[50] With 32 possible diastereomers, standard means of comparison of experimental and computed chemical shifts (e.g., mean absolute error/deviation) do not point to the correct

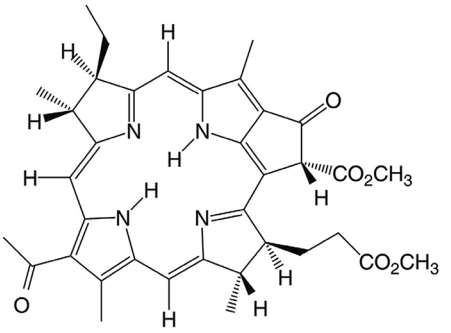

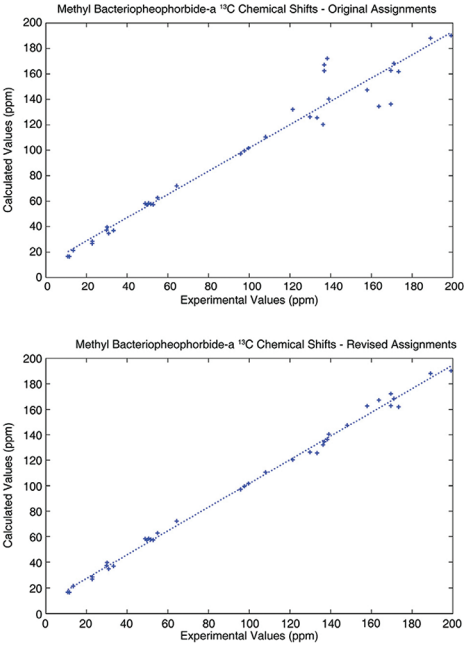

Figure 1. Original and revised ^{13}C chemical shift assignments for methyl bacteriopheophorbide *a*. The upper graph shows correlation of computed vs experimental chemical shifts based on original nuclei assignment and lower graph shows the same correlation based on the revised nuclei assignment. Plots are reproduced from data taken from ref 40.

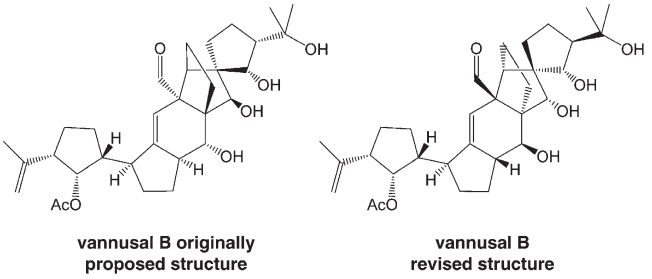

Figure 2. Original and revised structures for vannusal B (both arising from analysis of experimental NMR data).[49]

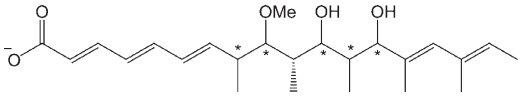

Figure 3. Ardisson's polyketide. Asterisks indicate the stereocenters that were varied in the analysis of all 32 possible diastereomers.[50]

isomer. However, the DP4 analysis indicates a strong match (approximately 85% probability) to the correct structure, with the remaining probability assigned to one other candidate isomer, even with the limited availability of experimental data in this case.

Also in the area of structure elucidation, we find examples of the use of computed chemical shifts for confirming the expected regio- or diastereoselectivity of a reaction[22,29,44,45,49−52,57−59] (which is particularly useful along a synthetic route when an unexpected result early in the sequence might otherwise not be discovered until much later), as well as for confirming the structure of complex natural products, which are occasionally misassigned even after obtaining a plethora of homo- and heteronuclear correlations.[32,33] One noteworthy example of the revision of a complex natural product, in part through comparisons

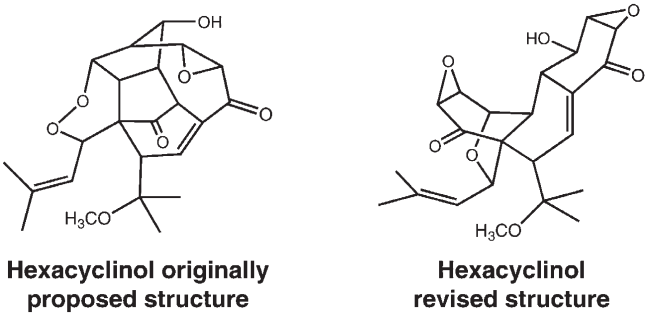

Figure 4. Originally proposed and revised structures of the natural product hexacyclinol.[60]

of computed chemical shifts to experimental data, is the case of hexacyclinol (Figure 4). The so-called "hexacyclinol dispute" began with the isolation of the natural product in 2002 and has involved two total syntheses and multiple rounds of analysis by means of computed NMR data.[60−62] The revised structure (Figure 4) was suggested by Rychnovsky on the basis of ^{13}C chemical shifts[62] and soon after, it was confirmed by total synthesis and crystallography.[63] After the correct structure was determined, Saielli and Bagno computed the ^{1}H spectrum and recomputed the ^{13}C spectrum of the original and revised structures to address the possibility of both structures having virtually the same NMR spectra; the ultimate conclusion was that they do not and the revised structure is correct.[60]

Many other examples of using computed NMR chemical shifts to aid the reassignment of structures (or to confirm proposed structures) have been reported.[24,25,30,53−56,64−73] We point out here that in some cases, a single, relatively simple NMR calculation may be sufficient to rule out a proposed natural product structure before it is put forth in the literature and/or before

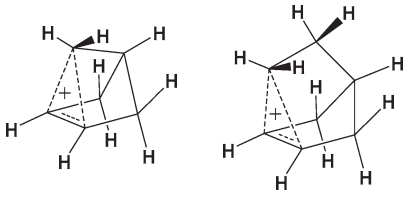

Figure 5. Nonclassical cations characterized using computed chemical shifts.

efforts toward a total synthesis are attempted. Also, although not falling into the category of quantum mechanical chemical shift calculations, readers may be interested in several automated structure elucidation techniques. These methods (often called "expert systems") utilize a variety of techniques to rapidly generate possible isomers and screen them against known NMR data in order to identify likely candidate structures for natural products and related compounds.[74,75]

NMR characterization of reactive intermediates is also useful, especially in cases where the structure and/or nature of bonding in these species are debated. Here researchers have turned toward theoretical NMR predictions to help resolve these debates. In one prominent set of examples, the cations depicted in Figure 5 were clearly shown to exist as delocalized, nonclassical structures (rather than two rapidly interconverting classical structures), in part on the basis of comparisons of computed ^{13}C and ^{1}H chemical shifts for both localized and delocalized species with those observed experimentally.[76,77] As mentioned earlier, carbocation structure studies were in fact the first practical applications of computed chemical shifts, and continue today to serve as important examples of the utility of these techniques.[8−10,18,78]

In another example, the structures of intermediates involved in the photosensitized oxidation of guanine derivatives were reassigned after comparison of computed chemical shifts to experimental shifts obtained at low temperatures (Figure 6).[79] As shown in Figure 6, computed ^{13}C chemical shifts for one isomer match experimental shifts much more closely than do those for the alternative isomer.

Other examples include the use of computed chemical shifts to examine unusual multicenter bonding arrays,[80] to help characterize host−guest systems[81,82] and to study numerous tautomerization[44,83−88] and conformational processes.[83−100]

Finally, computed chemical shifts that exist solely in the realm of theory, so-called nucleus-independent chemical shifts (NICS), have also found extensive application.[101,102] In this technique, chemical shifts are computed at any desired point in space in or around a structure of interest and are used to probe the shielding/deshielding properties of the structure in a way that is not normally accessible via traditional experiment. This technique has gained widespread use and acceptance as a valuable criterion for aromaticity (and antiaromaticity), and can be applied to molecules as well as transition state structures (e.g., for pericyclic reactions).

1.2. Basic Procedures

1.2.1. Molecule of Interest. NMR chemical shift calculations (not including the increment methods; see section 4.3.1) require several distinct steps. To begin with, a reasonable geometry for the molecule of interest needs to be obtained. This geometry can be found in a variety of ways, with perhaps the most common approach being an optimization routine with molecular mechanical, semiempirical, or quantum mechanical (wave function or density functional theory) methods. Snapshots from molecular dynamics simulations can also be used, and are commonly employed when consideration of explicit solvent molecules is

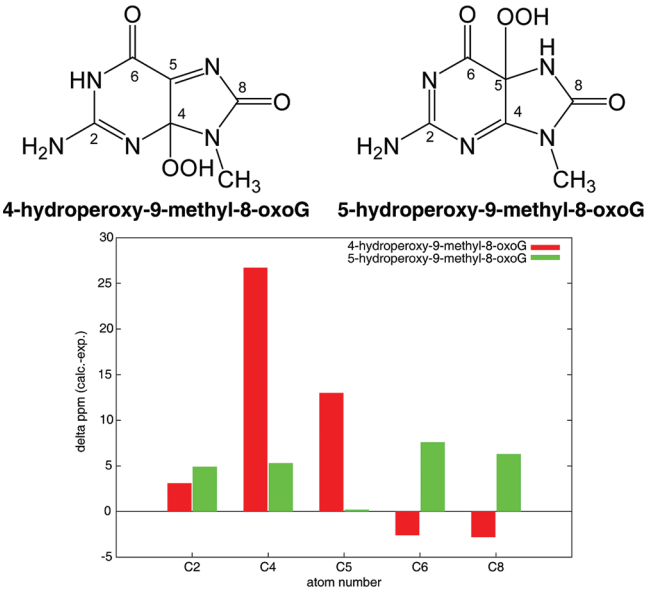

Figure 6. Comparison of computed [B3LYP/6-311+G(2d,p)//B3LYP/6-31G(d)] chemical shifts for two possible intermediates involved in a reaction of oxidized guanosine derivatives with experimentally observed shifts. The plot is reproduced from data taken from ref 79.

desired (see, for example, refs 39, 103, and 104). In certain cases (but not all, vide infra), a structure derived from experimental data can also be utilized.[105−108] The effects of geometry on NMR computations are detailed in section 4.1. Of further concern is the relatively long time scale of NMR experiments, which most commonly results in spectra that reflect a Boltzmann distribution of several conformations for the molecule of interest (as opposed to a single conformation; see section 2.3).

The second major step in calculating chemical shifts is to compute the NMR isotropic shielding constants (σ) for the various nuclei in the molecule. These calculations are almost always conducted with ab initio quantum mechanical methods, most commonly with density functional theory (DFT), perturbation theory (e.g., MP2), or higher-level post-HF methods [e.g., CCSD(T)].[109] It is important to note that the method chosen for computation of isotropic shielding constants need not have any direct connection to that utilized for the geometry optimization step. At this stage, common practice is to average the isotropic shielding constants for all nuclei that are related by symmetry (which should be identical to each other given tight enough convergence criteria in the calculations) and for nuclei that are experimentally indistinguishable due to free rotation around single bonds (for example, methyl protons). Diastereotopic or constitutionally heterotopic nuclei are generally not averaged unless they are known to be indistinguishable in the experimental spectrum.

1.2.2. Reference Compound. Once the computed isotropic shielding constants are in hand, they must be converted to a chemical shift (δ) value. Just as it is (implicitly) done experimentally, the chemical shift (δ_i) for ^{1}H and ^{13}C nuclei are (in general) obtained from subtracting the isotropic shielding constants for the nuclei in the molecule of interest (σ_i) from those of tetramethylsilane (TMS; σ_{ref}, see eq 1).

$$\delta_i = \sigma_{ref} - \sigma_i \quad (1)$$

Using TMS as a computational reference is a reasonable choice because of the simplicity and intuitiveness in doing so. Furthermore, while significant error may exist for any given method in the calculation of the shielding constants, using the exact same method to compute isotropic shielding constants for TMS and the molecule of interest will likely result in similar error for both. Thus, chemical shifts calculated in this way often benefit from a fair amount of error cancellation. That being said, the error cancellation is never perfect and the validity of this approach is dependent upon the correlation of the computed isotropic values to experimental chemical shifts, a feature that can vary widely across different computational methods (see section 4.3).[110,111] Furthermore, specific errors in computed ^{13}C isotropic shielding constants for the carbon atoms attached to silicon in TMS can adversely affect chemical shifts computed in this manner (see section 2.5).

Considering this issue and the fact that the experimental attributes for which TMS is chosen have no real significance for computed chemical shifts, it is often advantageous to consider alternate reference compounds. These may be chosen such that their nuclei bear more similarity to the nuclei in the compound of interest and therefore should benefit from more complete cancellation of error. As long as the experimental chemical shifts of the reference compounds are known, it is a trivial matter to convert chemical shifts computed in this manner into ones that are expressed relative to TMS by also incorporating the chemical shift of the new reference (relative to TMS; see eq 2).

$$\delta_i = \sigma_{ref} - \sigma_i + \delta_{ref} \quad (2)$$

In this equation, the chemical shift relative to TMS for each nucleus in the molecule of interest (δ_i) is determined from the computed shielding constants computed for the same nucleus type in the reference compound (σ_{ref}), the computed shielding constants for each nucleus in the molecule of interest (σ_i), and the known experimental chemical shift for the reference compound (δ_{ref}). This approach has indeed been put forth in the literature and demonstrated to have significant benefits.[70,72,112,113] The procedure is analogous to taking experimental NMR spectra with an internal standard other than TMS. For example, compounds of interest are often dissolved in some deuterated solvent, and the peak for this solvent is later set to the known chemical shift relative to TMS, thereby referencing the molecule of interest to TMS.

A logical extension to using a single reference compound other than TMS is to consider the use of multiple reference compounds. This was proposed in 2009 by Sarotti and Pellegrinet, and a significant improvement over chemical shifts calculated with any single reference compound was demonstrated.[114] For example, Table 1 summarizes the deviation in computed ^{13}C chemical shifts at several levels of theory from experimental values for a set of 50 organic compounds, using TMS as a reference compound and also using methanol as the reference for sp^3-hybridized carbons and benzene for sp- and sp^2-hybridized carbons [the multi-standard (MSTD) approach]. The only apparent trade-off here is the slight increase in complexity when processing data utilizing multiple reference compounds.

A third alternative actually obviates the need for any specific reference compound. With a linear regression approach (see section 3.6), if the computed isotropic shielding constants for a given computational method are plotted (*Y*-axis) against the known experimental chemical shifts (*X*-axis) for many compounds, then the (scaled—see ref 115) *Y*-intercept of the resulting best fit line represents (and in ideal cases is identical to) the computed isotropic value for TMS.[115−117] Among other benefits discussed in section 3.6, this approach allows for cancellation of errors in an average sense, based on a large collection of data rather than based on only one or a few specific compounds, and takes into account imperfect correlation between theoretical and experimental values, thus avoiding any specific error associated with a reference compound. In particular, Migda and Rys noted that subtracting computed ^{13}C isotropic shielding constants from TMS values resulted in mean absolute errors 2−3 times greater than when they used the intercept of a linear regression plot.[118] This approach does, however, require a substantial amount (a database) of reliable experimental and computational data. Furthermore, the computational data must be determined uniquely for any desired level of theory and must be recompiled any time the databases are modified. Linear regression approaches have been extensively applied to predicting ^{13}C chemical shifts[31,118−126] and to ^{1}H shifts as well,[111,116,117,120,126−128] although care must be taken for ^{13}C to avoid specific data that may adversely affect the quality of the linear regression (such as shifts for carbons attached to heavy atoms; see section 3.6).[110,129]

Table 1. Comparison of Errors in ^{13}C Computed Chemical Shifts for a Set of 50 Organic Compounds Determined via Comparison with TMS and Methanol/Benzene (MSTD)[a]

	average MAD		average RMSD	
level of theory	MSTD	TMS	MSTD	TMS
HF/6-31G(d)	3.2	3.9	8.6	11.0
HF/6-311+G(2d,p)	3.0	5.7	7.8	14.4
B3LYP/6-31G(d)	2.3	5.0	5.7	11.3
B3LYP/6-311+G(2d,p)	2.4	5.4	5.1	9.4
mPW1PW91/6-31G(d)	2.1	3.8	4.9	8.1
mPW1PW91/6-311+G(2d,p)	2.1	4.7	4.6	8.2

[a] Average errors are expressed in terms of mean absolute deviations (MAD) and root mean square deviations (RMSD). Data are reproduced from Table 3 in ref 114.

2. SOURCES OF ERROR

It has been noted frequently in the literature that uncorrected NMR chemical shift calculations, even when performed using some of the best computational methods, are associated with average errors of up to 0.4 ppm or more for ^{1}H shifts and up to 10 ppm or more for ^{13}C shifts, with outliers displaying even larger deviations.[114,116,125,130] These errors are clearly too large for many applications. There are many sources for such errors, and understanding these sources, at least at a basic level, is essential for their effective remediation.

2.1. Electron Correlation

Electron correlation refers to how each electron in a given system responds to every other electron in an instantaneous fashion, a behavior that is notoriously difficult to model computationally and that is the major focus of post-Hartree−Fock computational techniques. The fundamental Hartree−Fock (HF) method neglects specific correlation altogether in order to solve the wave equation, while modern methods such as density functional theory, perturbation theory (e.g., MP2), and coupled-cluster theory [e.g., CCSD(T)] use various approaches in attempts to account for correlation, none of which are exact

(although coupled-cluster methods come very close).[131] Inexact modeling of electron correlation results in an inaccurate description of the electron distribution in a system, which can ultimately lead to errors in computed geometries, nuclei shielding constants, and the resulting chemical shifts. Although there was some early success in predicting chemical shifts with the HF method, accuracy with this method depends strongly on cancellation of errors, and good treatment of electron correlation is now considered imperative for high accuracy chemical shift determination.[132] While electron correlation is always a factor, the magnitude of errors associated with its incomplete treatment depends heavily on the nature of the system being examined and the computational method being used. It should be noted that identifying systems that are expected to display significant correlation effects is not trivial. In fact, it has been shown that numerous common and simple organic molecules display significant electron correlation effects.[131,133−135]

2.2. Solvent and Other Intermolecular Interactions

A typical gas-phase calculation considers a molecule in a vacuum, completely isolated from any other molecules of its own kind or other types. In reality, of course, this is seldom the case in the experimental system, where the molecule interacts with others of its kind and/or solvent molecules. These interactions range from the exceedingly weak London dispersion interactions of a neutral, nonpolar molecule with a nonpolar solvent, to the strong H-bonding interactions of charged molecules with protic solvents. These interactions can affect computed molecular geometries and the calculation of shielding constants. Fortunately, from a practical standpoint, solvent effects on computed chemical shifts associated with organic compounds dissolved in common NMR solvents (such as $CDCl_3$) are often surprisingly small[129] and can be accounted for relatively easily. On the other hand, it can be exceedingly difficult to reproduce the experimental chemical shifts of acidic protons. This difficulty arises not only from challenges in modeling important intermolecular interactions that may be present but also from the fact that the experimental values themselves vary significantly depending on solvent, sample concentration, and the presence of trace amounts of water or other impurities. Furthermore, certain molecules (e.g., acetic acid and formamide) are known to exist in solution primarily as dimers held together by hydrogen bonding.[125] This and other (concentration dependent) aggregation behavior can lead to difficulties in predicting accurate chemical shifts.[116,125]

2.3. Conformational Mobility

NMR calculations are always performed on a single, static structure, that is, using one particular set of nuclear coordinates. However, many organic compounds enjoy extensive conformational freedom, and their experimental NMR spectra represent Boltzmann-weighted averages (determined by relative free energies) of the NMR properties of each accessible conformation at the temperature at which the experiment is conducted.[21,24,116,125,136] The need to take multiple conformations into account can sometimes be the single biggest hurdle one must overcome in order to access accurate chemical shifts (especially in terms of human, rather than computer, effort). Even just finding all relevant conformations can be an overwhelming task considering that the potential number of conformations scales exponentially with the number of rotatable bonds in a molecule. The chemist must decide whether to attempt to find them by inspection or to utilize computational techniques designed to survey possible conformations (in hopes of finding most, if not all, relevant conformers). On the other hand, the situation is not always as daunting as it may seem. In order to assess the extent to which conformational freedom must be taken into account, the chemist must ask two basic questions: (1) Are the various conformations under consideration accessible at the temperature of the NMR experiment? (2) Are chemical shifts expected to vary significantly over the accessible conformations? For the first question, one should keep in mind that Boltzmann statistics dictate that (at room temperature) a 1 kcal/mol difference in free energy corresponds to an ~85:15 ratio and 3 kcal/mol corresponds to a >99:1 ratio of two conformers. Therefore, many conformational minima may not contribute significantly to the experimental spectra, and the experimental spectra may in fact be dominated by the contribution from the global (in terms of conformational space) minimum. For the second question, while chemical shifts are generally (but not necessarily) sensitive to conformation, these effects can be quite localized. Thus, regions of conformational mobility in the molecule will not always affect the entire spectrum, and depending on the application at hand, one may only be interested in the chemical shifts for a particular substructure.

2.4. Rovibration Effects

As discussed above, NMR calculations are always performed on a static set of nuclear coordinates, which usually represents the computed lowest energy structure, with all bond distances at their equilibrium values. However, real molecules of course are constantly moving about $3N$ degrees of freedom, where N is equal to the number of nuclei. Translational movement can be safely neglected, but vibratory motion (which is inherently coupled to rotation) should not be ignored. In reality, an experimental NMR spectrum reflects average shielding properties from the vibrating and rotating molecule, not simply from the equilibrium geometry modeled by basic calculations.[23,26,112] Although this effect can be significant in terms of computed shielding constants (errors of up to 4.5 ppm for ^{13}C), this error is highly systematic and the effect on computed chemical shifts is typically much smaller, due to cancellation of error.[131,137] Furthermore, efforts to take rovibration explicitly into account require that properties be determined at various geometries surrounding the equilibrium geometry for each normal vibrational mode and therefore are challenging to implement and computationally expensive for anything but the simplest molecules.[26,130] A somewhat different approach utilizing zero-point vibrational corrections for computed ^1H shielding constants and chemical shifts has been developed by Ruud and co-workers.[137,138] However, unless extensive efforts have been made to reduce more significant sources of error, error from rovibration is often either handled in a general sense (e.g., empirical scaling; section 3.6) or simply accepted.

2.5. Heavy-Atom Effects

It is well-known that the calculation of isotropic shielding constants and chemical shifts for carbon atoms attached to halogens and other atoms of the third row or greater (and chemical shifts for heavy atoms themselves) are subject to higher than average errors, with the computed shifts always being too deshielded.[25,26,110,121,122,129,139−142] This observation has been firmly linked to the neglect of spin−orbit contributions from relativistic effects (many common DFT and perturbation methods do not include terms for these effects), along with a smaller contribution from electron correlation effects.[25,26,110,121,122,139,140,142,143] This so-called heavy-atom effect is proportional both to the number and size of heavy atoms attached to carbon and therefore does seem to be systematic in

nature.[121] Furthermore, there is very little cancellation of this specific error in chemical shift calculations when TMS is used as a reference. In fact, error in computed chemical shifts for carbon atoms can approach several dozen ppm when, for example, three chlorine atoms, or fewer bromine or iodine atoms, are attached to the carbon atom in question. Fortunately, this effect is highly localized and does not significantly affect the chemical shifts of other nearby carbon nuclei or nearby carbon-bound protons.[121] It should be noted, however, that protons directly attached to heavy atoms do experience this effect, and the resulting error can be greater than the entire proton chemical shift scale![26]

A heavy-atom effect of sorts is also observed for carbon atoms attached to silicon, phosphorus, and sulfur, although in these cases the effect is not as strongly linked to relativity, and electron correlation may play a bigger role than for halogens.[110,141] The heavy-atom effect for silicon makes tetramethylsilane (TMS) a poor choice as a reference compound for ^{13}C computed chemical shifts (see section 1.2.2), since the specific error in the computed isotropic shielding value for TMS carbon atoms is propagated into the computed chemical shifts for the molecule of interest.

3. METHODS FOR REDUCING ERROR

Many approaches to decreasing error in chemical shift calculations have been described in the literature. These approaches are not always related in a one-to-one fashion to the error sources discussed in section 2, as some efforts are aimed at specific problems while others are more general in nature and are effective at reducing systematic error from several sources at once. Methods that are aimed at specific problems include solvation modeling, conformational and vibrational averaging, and relativistic calculations for treating heavy-atom effects. One may also include in this grouping the various computational methods that strive to better capture electron correlation effects. On the other hand, approaches that seek to reduce systematic error in a global sense include empirically parametrized computational methods, linear regression methods, and the multistandard approach (see section 1.2.2). It is worth noting that a certain amount of overlap exists between these two broad categories. For example, the error that results from neglecting solvation effects is generally systematic and is thus amenable to improvement by solvation modeling techniques or the more general linear regression approach. In fact, perhaps with the exception of conformational freedom and intermolecular interactions, each source discussed above produces error that is mostly systematic in nature and therefore can be improved by several of the approaches that will be discussed in detail below.

3.1. Correlated Computational Methods

In the realm of quantum mechanical calculations, there are a variety of methods that account for electron correlation effects to varying degrees. On one end of the spectrum is the Hartree−Fock method, which only treats electronic interactions in an average manner, neglecting specific correlation effects completely. On the other end exists methods, such as coupled-cluster theory, that are highly adept (but still imperfect) at capturing these effects; however, coupled-cluster and related methods are often prohibitively demanding in terms of computational resources for all but the smallest of molecules. Somewhere in the middle of this spectrum lie density functional theory and perturbation theory, which utilize different approaches to account for correlation in an approximate manner. Specific details on the performance of these methods can be found in sections 4.1 and 4.3, but from a practical standpoint, few options today can compete with the DFT methods for providing good results at a reasonable cost. Therefore, in the absence of extensive computational resources and highly specialized experience, the use of DFT calculations along with the various methods described below is recommended for routine determination of computed chemical shifts.

3.2. Solvation Modeling

Another of the first areas often turned to for improving the accuracy of chemical shift calculations is solvation modeling, since a certain amount of error arises from running chemical shift calculations in the gas phase.[20,23,26,31,116,144,145] This error can result from neglect of solvation effects in both the geometry optimization and shielding constant calculations, although the error is not always as large as one might expect, especially for the relatively nonpolar and common NMR solvent, $CDCl_3$.

One simple approach to correcting for solvent effects in computed chemical shifts is to measure the experimental chemical shift for the computational reference compound in the desired solvent. The solvent-corrected computed chemical shifts can then be determined via gas-phase calculations by adding the experimental chemical shift for the reference compound (in solvent) to the computed gas-phase chemical shift. Note that this approach is conceptually the same as that described above in section 1.2.2 for utilizing alternate reference compounds in chemical shift calculations.

More commonly, however, some form of solvent modeling is utilized, and these approaches can be organized into two general groups. The first consists of the explicit or cluster methods, which model solvent effects by explicitly including solvent molecules around the compound of interest during the geometry optimization and shielding constant calculations.[20,26,145,146] This is perhaps the most intuitive approach, although significant challenges exist with respect to the proper choice and placement of solvent molecules. Further, the addition of extra atoms, as well as convergence problems associated with the presence of relatively weak interactions, dramatically increase the demand on computational resources. The resource problem is sometimes managed by using hybrid computational methods such as QM/MM [in which the compound of interest is treated with quantum mechanics (QM) and the solvent molecules with much less demanding molecular mechanics (MM)] or ONIOM (which extrapolates higher-level results from lower-level calculations via a layered approach).[147−149] The placement of explicit solvent molecules is sometimes facilitated by molecular dynamics (MD) simulations (applied only to the geometry calculation portion of chemical shift calculations).[20,103,112,146,150] In particular, MD can capture the various geometries associated with motions of the solvent molecules.

The second common approach to solvent modeling comprises the implicit methods. In these, solvent is modeled primarily as a dielectric continuum in which the molecule of interest resides in a cavity created by defining solvation volumes around each atom.[151] While somewhat less intuitive than the explicit approaches, these implicit approaches prove to be easier to use in practice and are much more commonly utilized for NMR calculations.[19,20,23,26,31,112,116,144−146,151−154] However, in choosing an implicit method, one is faced with a myriad of options with respect to the specific continuum model to use as well as the ways in which the solvation volumes are defined. The most common continuum models appear to be IEF-PCM (integral

Table 2. Comparison of Computed (B3LYP/6-311++G**) Chemical Shifts (ppm, relative to the corresponding nuclei in zwitterionic alanine) of Cationic and Anionic Alanine Utilizing Various Solvent Models[a]

	vacuum	PCM	point charge[b]	charge + PCM[c]	cluster (MD)	cluster (MD) + PCM	exptl
				Cationic Alanine			
N	−3.54	−3.32	−2.84	−3.89	−1.79	−1.82	−2.20
C′	1.79	−1.04	−1.17	−1.24	−1.42	−1.80	−1.77
C^{α}	3.12	−1.38	−0.44	−1.53	−0.23	−1.86	−3.11
C^{β}	−3.09	−2.60	−1.68	−2.42	−0.87	−1.30	−0.83
H^{α}	0.67	0.075	0.65	0.70	0.62	0.75	0.37
H^{β}	0.51	0.25	0.32	0.027	0.28	0.22	0.08
MAD	2.35	0.98	0.88	0.99	0.69	0.44	--
				Anionic Alanine			
N	−12.97	−11.62	−8.28	−10.65	−8.96	−8.34	−6.60
C′	2.48	0.98	0.92	1.03	0.47	0.77	0.93
C^{α}	14.96	12.71	12.87	12.57	11.53	10.28	8.94
C^{β}	3.03	4.08	3.73	4.49	3.03	3.11	4.25
H^{α}	−0.97	−0.90	−0.73	−0.88	−0.56	−0.63	−0.48
H^{β}	−0.63	−0.43	−0.53	−0.33	−0.40	−0.28	−0.26
MAD	2.67	1.60	1.11	1.41	1.14	0.76	--

[a] Data are adapted from Table 2 in ref 146. [b] TIP3P partial atomic charges; see ref 146 for details. [c] Point charges[b] and PCM solvent continuum model.

equation formalism-polarizable continuum model, or just PCM) and CPCM (conductor-like polarizable continuum model) with UFF, UAHF, or UAKS radii for solvation volumes.[151,155−160]

In a representative study,[146] Dračínský and Bouř analyzed the effect of various solvent models on the chemical shifts of protonated/cationic and deprotonated/anionic forms of alanine (relative to the zwitterionic form) in water. As shown in Table 2, the best results were obtained using a combination of molecular dynamics (explicit solvent model) and PCM (implicit solvent model), demonstrating the value of each in capturing solvent effects of charged systems in a hydrogen-bonding solvent.

To the best of our knowledge, a systematic study of the various methods and variables involved in modeling solvent effects for NMR chemical shift calculations has not been reported, although various aspects of solvation modeling have been examined in the context of NMR calculations.[144,146,152] In fact, due to the sheer number of variables involved in solvent modeling and the anticipated system-dependence of the results, it is probably unreasonable to expect any such study to produce a bottom-line answer as to the best approach. Our recommendation for a dependable and straightforward approach to reducing error associated with solvent effects in routine chemical shift calculations (based on literature reports as well as our own unpublished results), is to utilize the PCM, CPCM, or SMD continuum methods with UFF, UAHF, or UAKS radii in the single-point calculation of NMR isotropic shielding constants. If feasible, the same methods may also be employed in the geometry optimization calculations, especially if the geometries in question are suspected to be sensitive to solute−solvent interactions. Finally, pairing solvent modeling with a linear regression approach (section 3.6) will likely further improve accuracy by reducing remaining systematic error.

3.3. Conformational Averaging

Depending on the nature of the system of interest, conformational freedom may dictate the need for extensive conformational searches and numerous mid- to high-level free energy calculations (see section 4.1.2), or the absence of significant conformational freedom may make such calculations irrelevant. It is the chemist's task to determine whether the system falls into one of these two categories or somewhere in between. Assuming that multiple low-energy conformations are possible, the chemist must then decide how to locate them. If the compound has only a few rotatable bonds, then the relevant conformers can likely be located by simple inspection, meaning the chemist can simply make educated guesses as to the geometries of all conformers and then run them through some sort of geometry optimization process (see section 4.1). If the compound has numerous rotatable bonds, however, then the chemist may elect to locate them via an automated searching technique.

Automated conformational search techniques typically rely on molecular mechanics or semiempirical methods to conduct molecular dynamics and/or Monte Carlo[161] calculations that can quickly search a large subsection of conformational space for a molecule and locate candidate local minima structures within a given energy window. There are many programs available to perform such a search, and interested readers are directed to review articles on that topic.[22,161−164] Specific programs used recently for NMR calculations include Spartan,[45,58,62,68] Macromodel,[50,52,96,104] Hyperchem,[84,95,165] INSIGHT II,[24,54] PCMODEL,[93] CHARMM,[166] and TINKER.[118] Many medicinal chemistry software packages and programs for computerized docking of ligands to protein targets also provide the ability to conduct conformational searches.[167−169]

Another option for locating conformers involves running relaxed or rigid potential energy surface scans (at any desired level of theory) around the various rotatable bonds in the molecule of interest.[29,170] These scans can include simultaneous rotation around several single bonds and can reveal conformer candidates in much the same way Monte Carlo searches can. Further, these scans often utilize software that can also be used to run geometry optimization and NMR calculations.

Note that the structures found by conformational searches are almost always subsequently refined with a quantum mechanical

method such as HF, DFT, or a higher-level method in order to obtain more accurate geometries and relative energies. Thus, it should make little difference in the end result which program is used to find the candidate conformers, as long as the conformational space is thoroughly sampled.[171]

Once candidate conformers have been located and refined, a Boltzmann analysis is used to determine the relative contribution each structure makes to the overall NMR spectrum. This is where it becomes important to have accurate relative free energies for the relevant conformers. In fact, while reliable geometries can often be determined with relatively inexpensive methods,[34,47,50,53,54,62,116,117,120,125,172] the need for accurate free energies may dictate the use of a higher level of theory and/or larger basis set (see section 4.1). The computed free energies along with an appropriate value for temperature are fed into the Boltzmann equation, two useful adaptations of which are given below (eqs 3 and 4).[120,144] Eq 3 expresses the abundance ratio of conformer i relative to conformer j using the computed free energies (G_i and G_j on a per-particle basis), the temperature, and the Boltzmann constant. Equation 4 expresses the overall computed chemical shift (δ) of a given nucleus using the computed chemical shift of that nucleus for each conformer (δ_i) and the computed free energies (G_i and G_j of all conformers on an absolute molar basis, i.e., in units of energy/mol), along with the temperature and molar gas constant. Note that eq 4 can easily be applied to the computed isotropic shielding constants (instead of chemical shifts) and can be adapted to work with relative (instead of absolute) free energies.[52] Either equation can also use per-particle or molar energies depending on whether the Boltzmann or molar gas constant is used. Equation 3 provides a quick way to assess whether or not a given conformer is a significant contributor to the overall NMR spectrum, based on its free energy relative to that for the lowest energy conformer, while eq 4 allows for the actual calculation of the conformationally averaged shielding constants and/or chemical shifts (see section 4.1.2). The ultimate goal for the conformational search is to locate all conformers that contribute to the experimental spectrum; in practice, this means all unique conformers that exist within a 2.5−3.0 kcal/mol free energy window, relative to the lowest energy conformer (see sections 2.3 and 4.1.2). It is important that the NMR parameters for all conformers (not just a representative set) within this window be computed and averaged according to the equations below.

$$\frac{P_i}{P_j} = e^{(G_i - G_j)/k_B T} \quad (3)$$

$$\delta = \sum_i \frac{\delta_i e^{-G_i/RT}}{\sum_j e^{-G_j/RT}} \quad (4)$$

3.4. Vibrational Averaging

As mentioned above (see section 2.4), efforts to explicitly reduce errors in NMR calculations due to rovibratory effects are both very expensive and technically demanding,[26] even with current techniques and equipment. Fortunately, errors due to neglect of rovibratory effects are largely systematic and are relatively small for computed ^{1}H and ^{13}C chemical shifts.[131] It should be noted, however, that rovibratory effects can be much more significant for absolute chemical shielding constants, for nuclei other than ^{1}H and ^{13}C, and for the calculation of spectroscopic properties other than chemical shifts.[23,26] Leading references to techniques for explicitly accounting for rovibratory effects, which range from classical dynamics to full quantum mechanical treatments, can be found in refs 23, 26, 112, 131, 173, and 174.

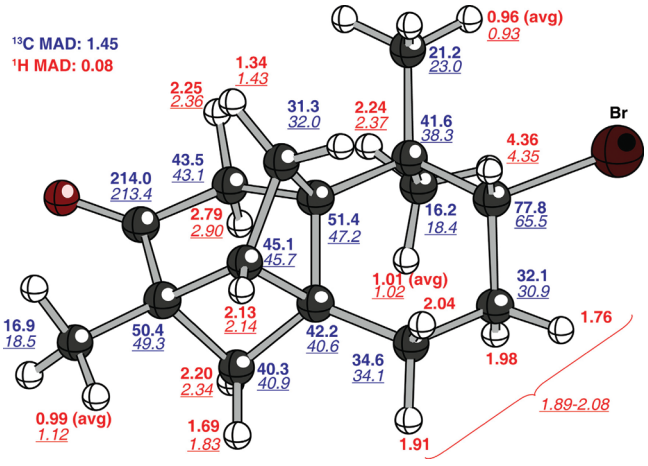

Figure 7. Computed [CPCM(UAKS)-(GIAO)mPW1PW91/6-311+G(2d,p)//B3LYP/6-31+G(d,p), scaled; see section 3.6] ^{1}H (red) and ^{13}C (blue) chemical shifts (ppm, relative to TMS) for aplydactone. Computed shifts are in bold text and experimental shifts[175] are in *underlined italics*.[176]

3.5. Heavy-Atom Calculations

The heavy-atom effect errors discussed in section 2.5, being systematic in nature and being rooted in relativistic and electron correlation effects, are amenable to improvement in several ways. First, however, one should remember that these effects are also highly localized and typically only affect the chemical shifts of carbon atoms directly attached to one or more heavy atoms. Consequently, if a researcher is interested, for example, in assigning the structure of a complex natural product possessing a single halogen atom, it may be quite reasonable to accept that the chemical shift for one carbon atom may be off by a significant amount and forego any additional efforts to reduce this error. The highly localized nature of heavy-atom effects in organic molecules is demonstrated by the data collected in Figure 7. Here, computed ^{1}H and ^{13}C chemical shifts, without any corrections for heavy-atom effects, for aplydactone,[175] a sesquiterpenoid natural product bearing a single bromine atom, are shown.[176] In this example, we can see that the ^{13}C chemical shifts are all reproduced quite accurately, with the sole exception of that for the carbon atom to which the bromine is bonded (computed = 77.8 ppm, actual = 65.5 ppm). Note that there appears to be no adverse impact on the computed chemical shift for the hydrogen atom attached to the same carbon.

This being said, one way to improve the computed chemical shifts of heavy-atom-bound carbon atoms is to utilize a method that better captures electron correlation effects, such as MP2 or higher-level methods along with correlation-consistent basis sets (see section 4.3). This will likely result in significant improvement for carbon atoms attached to sulfur or phosphorus as well as to halogens, although the improvement is expected to be greater for sulfur or phosphorus.[25,122,141] Further improvement requires the use of methods that determine relativistic spin−orbit corrections.[139,142] In the context of ^{13}C NMR spectroscopy, these include the ZORA formalism available, for example, through the

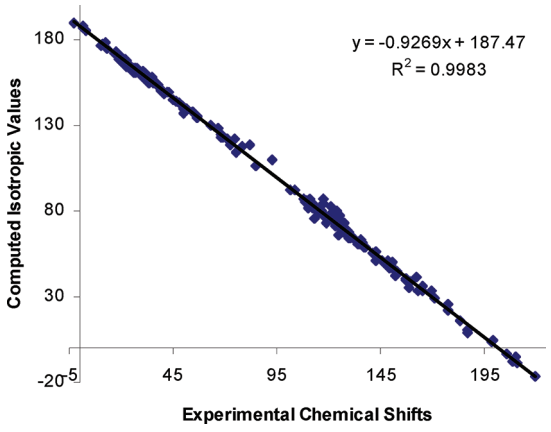

Figure 8. Sample correlation plot for computed ^{13}C NMR data for a large set of small organic compounds.

Amsterdam Density Functional (ADF) code.[122,140,150,177] In fact, Bagno et al. observed the best results when adding a ZORA-derived spin−orbit correction to MP2-derived shielding constants, even though the two types of data were derived from very different computational methods.[122] Other literature reports discuss the theoretical aspects of these relativistic calculations.[20,26,141,143,178,179]

Another option for improving chemical shift calculations with heavy-atom errors is to utilize a linear regression method, as discussed in section 3.6. Due to the systematic nature of heavy-atom effects, they are amenable to improvement via this approach, provided that the linear regression data consists of nuclei similar to the nucleus of interest. That is, a linear correlation correction to carbon nuclei attached to a given number of bromine atoms, for example, should be derived from empirical data for other carbon nuclei attached to the same number and type of halogen atoms. In fact, this approach has been demonstrated specifically for such cases.[121,129]

3.6. Linear Regression

Perhaps the most general approach to error reduction is empirical scaling, namely, the application of corrections derived from linear regression procedures.[28,31,50,111,115−129,172] When sufficient experimental data is available, plots of several varieties may be generated; these include computed chemical shifts vs experimental chemical shifts, computed isotropic shielding constants vs experimental chemical shifts, or computed isotropic shielding constants vs experimental isotropic shielding constants. For all types of plots, linear fits are usually observed. The quality of the fit reflects the extent to which the computational method is able to produce data free from random error, and the extent to which the slope of the correlation line deviates from unity is a measure of the overall systematic error.

The major benefit to this analysis is that the slope can be used as a scaling factor to correct the computed chemical shifts for systematic error. It has been noted that such a procedure is able to reduce error from sources such as solvation effects, rovibratory effects, and other method limitations, all at one time.[118] Furthermore, if plots of the computed isotropic shielding vs experimental chemical shifts variety are generated and analyzed, the γ-intercept provides a convenient alternative for a reference value from which the computed isotropic values can be converted to chemical shifts relative to TMS.[116,117]

As an example of this technique, consider the data plotted in Figure 8, which shows the linear fit for computed ^{13}C isotropic shielding constants plotted against corresponding experimental chemical shifts for a large set of small organic molecules. In this example (see the Appendix for details), a tight correlation indicated by the high R^2 value of 0.9983 indicates very little random error associated with this method (in general, one should expect a value of no less than 0.995 for a well-performing method). However, the slope of −0.9269 (a significant deviation from the ideal value of −1) indicates that this particular method exhibits a fair amount of systematic error. In our experience, a slope that deviates from −1 by no more than ±0.05 is indicative of a well-performing method, however as long as there is little random error, the effects of any degree of systematic error can be reduced by this scaling procedure. Using the linear regression data, scaled computed chemical shifts for other molecules analyzed at the same level of theory could be determined with eq 5, where δ is the computed chemical shift determined from σ (the computed isotropic value for a given nucleus).[180,181]

$$\delta = \frac{\text{intercept} - \sigma}{-\text{slope}} \tag{5}$$

In practice, such a plot can be generated for ^{1}H and ^{13}C calculations for any given level of theory using either a sufficiently large set of organic molecules containing a variety of structural features as input, or using a smaller set of molecules that are similar to the molecule(s) of interest (although one must be careful that the data set is not too small). The main requirement is the availability of reliable experimental chemical shifts, preferably all determined in the same or similar solvents. In addition, utilizing a test set of molecules whose chemical shifts can be modeled effectively by analyzing only a single conformer greatly simplifies the task of generating the correlation plots. Beyond these considerations, it is important when choosing ^{13}C data to be wary of heavy-atom effects. As discussed in detail above, the neglect of relativistic effects for molecules bearing halogen and other third row and higher elements can result in systematic errors that can adversely affect linear correlations derived mainly from, and intended for, compounds lacking these heavier elements.[110,129] Numerous examples of training (or test) sets have been reported in the literature.[114,116,117,119−121,125−127,129,141]

Once linear regression parameters have been determined for a given level of theory, it is good practice to test them on a second set of molecules with known chemical shifts in order to confirm their ability to reproduce chemical shifts beyond the input set before applying them to chemical shift calculation on the molecule of interest.

A somewhat more elaborate approach to linear scaling has been implemented in the software package Spartan'10. Here, corrections to the computed chemical shifts are made based on numerous parameters related to bond counts and bond orders (as determined by the Natural Bond Order analysis).[182] Spartan'10 has implemented scaling schemes for both B3LYP/6-31G* and EDF2/6-31G* methods. The linear regression data set for each of the methods is quite large, e.g., for EDF2/6-31G* it comprises some 8000 sp^3 centers, 6200 sp^2 centers, and 450 sp centers (for B3LYP/6-31G* it is ∼800, 1500, and 100 sp^3, sp^2, and sp centers, respectively).

While the above empirical scaling approaches may be "impure" from a theoretical perspective, their usefulness is undeniable. As mentioned earlier, uncorrected error in computed chemical shifts can average 0.4 ppm or more for ^{1}H and up to 10 ppm or more for ^{13}C with common and affordable computational

Table 3. Average Errors in Computed Chemical Shifts for the *β*-Lactam Shown Below, Computed at Various Levels of Theory[a]

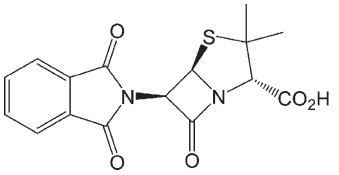

	^{13}C		^{1}H	
method	ME	MUE	ME	MUE
WC04	−1.1 (−1.7)	2.9 (3.3)	−0.02 (−0.15)	0.23 (0.16)
WC04	8.0 (0.3)	8.0 (3.1)	0.01 (−0.06)	0.10 (0.06)
HF	5.9 (−4.7)	7.5 (4.8)	0.10 (−0.09)	0.30 (0.14)
B3LYP	7.9 (−0.3)	7.9 (2.4)	0.11 (−0.07)	0.15 (0.07)
PBE1	6.7 (−0.6)	6.7 (2.2)	0.14 (−0.05)	0.19 (0.05)
mPW1PW91	6.8 (−0.6)	6.8 (2.2)	0.13 (−0.05)	0.18 (0.06)

[a] The geometry was determined at the B3LYP/6-31G(d) level of theory, the NMR calculations utilized a 6-311+G(2d,p) basis set, and all calculations included an implicit chloroform solvent model. The left-hand values are unscaled chemical shifts and the righthand values in parentheses are empirically scaled. ME refers to mean error and MUE refers to mean unsigned error. Data are adapted from Table 5 in ref 120.

techniques.[114,116,125,130] With the benefit of empirical scaling, however, average errors can drop below 0.1 ppm for ^{1}H and two ppm for ^{13}C for the same systems (essentially experimental precision).[28,116,118,119,125,182] For many purposes, this amount of improvement is sufficient to allow the successful application of computed chemical shifts. Without empirical scaling, this same degree of improvement might only be realized through the use of very high levels of theory and elaborate efforts to explicitly account for solvation, rovibratory effects, electron correlation, and other sources of error (vide supra), techniques that are not readily accessible to many researchers. On the other hand, for ^{13}C chemical shifts, it has been demonstrated that the use of one or more alternate reference compounds can sometimes produce results comparable to those achieved through empirical scaling, presumably due to improved cancellation of error (see section 1.2.2).[112,114]

3.7. Empirically Parametrized Computational Methods

A different approach to removing systematic error in an empirical fashion has been put forth by Hoye, Cramer, and coworkers.[120,136] These authors began with the popular B3LYP density functional method and systematically varied the five weighting parameters that define exchange and correlation energies while assessing the ability of each method to reproduce known chemical shifts of 43 organic molecules (in $CDCl_3$). This analysis resulted in two modified versions of B3LYP (WP04 for ^{1}H and WC04 for ^{13}C) that predict chemical shifts with greater accuracy than does the original B3LYP (as well as two other common functionals: PBE1 and mPW1PW91). The authors also noted that with linear regression analyses, the tested functionals converged upon a consistent level of accuracy. This is evidenced by the data in Table 3, computed for the heteroatom-rich molecule shown. Other functionals parametrized to reproduce absolute shielding constants (in contrast to chemical shift values) have also been reported.[183]

Table 4. Mean Absolute Deviation (MAD) of Various Methods from Experimental Bond Distances, Angles, and ^{13}C Chemical Shifts[184]

	MAD		
method	bond distance (Å)	bond angle (deg)	^{13}C δ (ppm)[a]
HF/6-31G(d)	0.011	0.48	2.36
BLYP/6-31G(d)	0.015	0.64	5.80
B3LYP/6-31G(d)	0.007	0.58	4.43

[a] (GIAO)B3LYP/6-311+G(2d,p) NMR calculations using the geometry in the method column.

3.8. Summary of Best Practices to Eliminate Error

In this section, we have discussed several methods for reducing error in computed chemical shifts. The take-home message is that average errors on the order of 0.1 ppm for ^{1}H and a few ppm for ^{13}C (approximately 1% of their respective chemical shift ranges) are readily attainable through a variety of techniques. While advanced approaches such as high-level coupled-cluster calculations and explicit consideration of solvation, rovibratory, and relativistic effects can lead to extremely accurate results, it has been demonstrated that more general and accessible approaches to systematic error reduction can do so as well. For the organic chemist who is not an expert in computational techniques and does not have access to extensive computational resources, the use of DFT calculations employing implicit solvation models along with linear regression analysis (see the Appendix) and/or alternative reference compounds and/or empirically parametrized functionals permits access to high-quality predicted chemical shifts that can be used to tackle a multitude of problems.

4. COMPUTATIONAL METHODS

This section surveys technical aspects of computing NMR shielding constants and associated chemical shifts—from methods for computing geometries, to methods for quantifying the interaction of a molecule with a magnetic field, to the model chemistries and basis sets used to determine the isotropic shielding constants (and associated chemical shifts).

4.1. Methods for Determining Geometry

The first, and often the most time-consuming, step in an NMR calculation involves determining the three-dimensional structure of the molecule in question. This process is often quite simple to implement; however, if multiple conformations need to be considered, or if some gas-phase artifacts appear (requiring solvent approximations), then the procedure becomes more complicated.

4.1.1. Molecules with a Single (Contributing) Conformation. If the molecule of interest has only one conformation contributing to the NMR spectrum (as defined in section 4.1.2), then only a single geometry optimization (in principle) is necessary. The accuracy of several common methods has been evaluated and the variation in equilibrium bond lengths between them is remarkably low (often less than 0.01 Å),[184−191] at least for structures lacking unusual bonding features. For example, in 2007, Zhang et al. compiled optimized bond lengths and angles for 18 small organic molecules for which experimental bond distances and angles were also available (Table 4)[184] and found that even HF can reproduce bond distances to about 0.01 Å resolution and

Table 5. Correlation Coefficient and Standard Deviation of ^{11}B Chemical Shift Data[a] as a Function of Geometry for Various Boranes and Carboranes[190]

geometry	linear regression correlation coefficient	standard deviation of chemical shift (ppm)
experimental[b]	0.972	5.6
HF/3-21G	0.976	5.6
HF/6-31G(d)	0.985	4.2
MP2/6-31G(d)	0.993	3.0

[a] NMR data was computed using the IGLO method and the DZ basis set. [b] Methods for obtaining experimental geometries include electron/X-ray diffraction and microwave spectroscopy.

bond angles to approximately 0.5°. Herein, however, we are concerned with how the underlying geometry affects the computation of chemical shifts. Also displayed in Table 4 are mean absolute deviations of chemical shifts [computed with (GIAO)-B3LYP/6-311+G(2d,p) using the respective geometries]. Although the HF/6-31G(d) method for optimizing the geometry resulted in bond distances off (on average) by just over 0.01 Å and bond angles off by approximately 0.5° (not the closest to experiment of those methods in Table 4), it was found to best reproduce ^{13}C chemical shift data for the test set used, indicating that small errors in geometry can significantly affect computed chemical shifts. Nonetheless, the geometries calculated with all three methods still provided useful estimates of ^{13}C shifts.

The lack of a one-to-one correspondence between a method's ability to reproduce experimental geometry and chemical shift data is echoed in a 1992 report by Bühl and Schleyer.[190] In their report, several methods were used to compute structures of boranes and carboranes, and chemical shift data were computed on the basis of the various optimized geometries, as well as those obtained from experiment (determined by various methods). Their findings are summarized in Table 5. It is apparent from Table 5 that use of the experimental geometries produced chemical shift data of worse accuracy than even the very cheap HF/6-31G(d).[190]

Other studies have found that for the computation of chemical shift data, the HF/6-31G(d) method for geometry optimization produces better results than even some more modern DFT methods.[119,172] However, HF neglects electron correlation, and so its use has been limited to structures lacking highly delocalized bonding arrays. In 1999, Dokalik et al. reported that inclusion of electron-correlation effects (using either MP2 or B3LYP) can improve correlations between computed and experimental ^{1}H and ^{13}C isotropic shielding constants for their test set of nitrogen containing organic (and mostly aromatic) compounds (see Table 6).[192] Data in Table 6 suggest that B3LYP- and MP2-optimized geometries provide similar deviations in computed chemical shifts, a trend noticed by others in the computation of both ^{1}H and ^{13}C chemical shifts.[117,129] Efforts to include electron correlation using a more rigorous treatment—coupled-cluster calculations—showed little improvement over geometries determined with MP2 (see Table 7).[131]

However, there are cases that exist in which only a rigorous treatment of the molecular geometry gives accurate NMR data. In 2011, Harding et al. showed that 1-adamantyl cation is just such a case.[18] It was also noted that a better treatment of electron correlation [namely, the use of CCSD(T)] is necessary to accurately describe vinyl cations (see Table 8).[133]

Table 6. Correlation Coefficient and Standard Deviation of ^{1}H and ^{13}C Isotropic Shielding Constants[a] Determined from Various Geometries (^{1}H in normal text, ^{13}C in *italics*)[192]

method	linear regression correlation coefficient[b]	standard deviation of isotropic shielding constant (ppm)
HF/6-31G(d,p)	−0.9826	0.14
	−0.9930	*1.6*
MP2/6-31G(d,p)	−0.9869	0.12
	−0.9955	*1.3*
B3LYP/6-31G(d,p)	−0.9848	0.13
	−0.9960	*1.2*

[a] NMR data computed with (GIAO)B3LYP/6-311++G(d,p) method. [b] Correlation is to chemical shift data obtained in $CDCl_3$.

Table 7. MAD of ^{13}C Isotropic Shielding Constants[a] Determined from Various Geometries of 19 Small Organic Molecules[131]

method	MAD (ppm)
MP2/cc-pVTZ	5.99
CCSD(T)/cc-pVTZ	5.90
CCSD(T)/cc-pVQZ[b]	5.78

[a] NMR data computed with the (GIAO)CCSD(T)/qz2p method. [b] Data only available for a 13 molecule subset.

Table 8. MAD of ^{13}C and ^{1}H Chemical Shifts[a] for 1-Adamantyl Cation Computed with Various Geometries[133]

method	MAD	
	^{13}C chemical shift (ppm)	^{1}H chemical shift (ppm)
HF-SCF/cc-pVTZ	7.95	0.31
MP2/cc-pVTZ	5.53	0.31
CCSD(T)/cc-pVTZ	4.83	0.24

[a] NMR data computed with (GIAO)MP2/qtzp method.

The low computational cost of density functional theory (DFT) has made it an immensely useful tool in electronic structure theory. In 2009, Sarotti and Pellegrinet compared two popular functionals (B3LYP and mPW1PW91) in their ability to determine geometries (as measured by ^{13}C NMR mean absolute deviations).[114] They found that B3LYP produced lower MADs for sp^2-hybridized centers than did mPW1PW91; however, the opposite was found for sp^3-hybridized centers. Further, the effect of basis sets for optimizations was systematically investigated and the 3-21G set was found to be too small, while the 6-31G(d), 6-31G(d,p), and 6-31+G(d) basis sets all produced similar MADs.[114]

Cheeseman et al. have previously recommended that geometry optimization with the B3LYP hybrid DFT functional (or other, similar functional), paired with a basis set of at least 6-31G(d) quality is generally sufficient.[193] We tend to agree with this recommendation.

4.1.2. Multiple Conformations. The somewhat long time scale of NMR experiments allows low-energy processes such as conformational averaging to take place during an experiment; therefore, many experimentally determined chemical shifts correspond to conformationally averaged values. In a practical sense,

two criteria determine if including alternative conformers will increase the likelihood of accurately reproducing (or predicting) experimentally determined NMR chemical shifts: (1) The difference in energy between the lowest energy conformation and alternatives is less than approximately 3 kcal/mol. (2) There is a difference in isotropic shielding constants for the conformers that meet criterion 1.

If the first criterion is not met, then Boltzmann distribution (see section 3.3) considerations dictate that no significant percentage of the conformer in question will be present (a difference in free energy of 3 kcal/mol at 25 °C corresponds to ~1% of the higher energy conformer). The second criterion simply states that averaging two structures with the same or similar chemical shifts results in an NMR that is essentially unchanged. Looking at the two criteria, it becomes apparent that both the geometry of each conformer and the relative energy become important.

Several reports assess the performance of various methods for determining kinetic (transition state structure relative to starting structure) and thermodynamic (two minima relative to each other) relative energies.[194−198] In 2008, Schwabe and Grimme reported that the B3LYP/TZV(2df,2pd) method results in a mean average deviation of 2.29 kcal/mol for the thermodynamic relative energies of 34 organic isomerization reactions.[194] A MAD of 2.29 kcal/mol is one of the many reasons why there is a large distaste for some functionals, such as B3LYP. Such a large MAD would certainly adversely affect Boltzmann distribution calculations relied upon for conformational averaging. Fortunately, many of the effects that make large contributions to error are systematic in nature, and therefore when conformers are compared much of this error cancels out.[199]

In 2006, Wiitala et al. examined 160 conformers of 43 molecules and found B3LYP/6-311+G(2d,p) free energies computed at B3LYP/6-31G(d) geometries to be adequate for Boltzmann distribution calculations.[120] In 2008, Branca et al. surveyed several basis sets for computing relative free energies of the four conformations of *S*-3-(1-naphthoyl)-4-isopropyl-2,2-dimethyloxazolidin-5-one;[144] this was transformed into relative ratios of the conformers and that data appears in Table 9. From Table 9, it is apparent that conformer 1 is overly emphasized in the relative ratio. It is important to note that increasing the size of the basis set [from the smallest 6-31G(d) basis set studied] improves the ratio, but error still persists.

We recommended that free energy calculations employing a double-ζ (or better) quality basis set with diffuse and polarization functions [such as 6-31+G(d,p)] are used when considering multiple conformations.

Table 9. Computed and Experimental Relative Ratio of the Four Conformers of *S*-3-(1-Naphthoyl)-4-isopropyl-2,2-dimethyloxazolidin-5-one (computed from eq 3; based on ΔG at −63.15 °C, computed using B3LYP)[144]

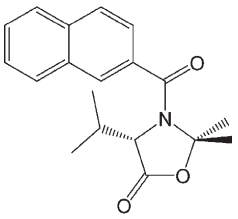

method	% conformer 1	% conformer 2	% conformer 3	% conformer 4
6-31G(d)	85.5	13.9	0.6	<0.1
6-31+G(d)	78.9	20.4	0.7	<0.1
6-31++G(d)	78.0	21.3	0.7	<0.1
6-311G(d)	83.9	15.4	0.6	<0.1
6-311++G(d)	78.2	21.1	0.6	<0.1
pSDD	72.5	26.7	0.8	<0.1
experimental	61.0	34.0	4.3	0.7

4.2. Overcoming Gauge Dependence

Ab initio computation of NMR chemical shifts requires accurate treatment of the interaction of an external magnetic field with the molecular Hamiltonian. The necessary use of finite basis sets results in a dependence on the origin (or "gauge") of the magnetic field vector; this is commonly referred to as the "gauge problem"[4,200] (for a thorough, technical discussion of the gauge problem, see ref 4). The first methods for computing magnetic properties of molecules involved a coupled-perturbed Hartree−Fock (CPHF) approach that required large basis sets in order to prevent gauge dependence.[201] To overcome this problem, "gauge-invariant" methods are now commonly used. Some of these methods include the individual gauges for atoms in molecules (IGAIM),[201] the continuous set of gauge transformations (CSGT) and the related continuous set of damped gauge transformations (CSDGT),[202] the individual gauges for localized orbitals (IGLO),[6,7] the local origin/localized orbitals (LORG),[173] and the gauge-including atomic orbital (GIAO)[203,204] methods.

Despite the wide variety of methods available, two dominate as the most commonly used methods. The GIAO method is preferred in most cases, since it has been noted that smaller basis sets can be used with this approach (when compared to the other methods).[193,205] The success of GIAO may also be attributed to its rapid incorporation into quantum chemical packages. However, GIAO is only available for use with certain density functional methods (GGAs and hybrid GGAs). When GIAO is not available (i.e., for meta-GGAs and hybrid meta-GGAs), then CSGT is usually preferred. It has been reported that GIAO and CSGT give similar results if large enough basis sets are used.[193] A more current variation on the CSGT method has been reported, namely, the "continuous transformation of the origin of the current density" (CTOCD) approach.[206] Within this formalism, one finds CTOCD-DZ (also referred to as ipsocentric)[207,208] and CTOCD-PZ (also referred to as allocentric),[209] where the diamagnetic or paramagnetic contributions to the total current density are annihilated, respectively.[210] This formalism has yet to become solidly adopted in the routine computation of NMR properties for organic molecules.

4.3. Model Chemistries for NMR Calculations

4.3.1. Increment-Based Methods. One of the conceptually simplest ways to predict NMR chemical shifts is through an increment-based method. In such a method, the molecule of interest is compared to a library of compounds with known chemical shifts. Each nucleus is assigned a chemical shift from the library of known compounds on the basis of its unique environment. Such a prediction scheme has been carried out by hand for years,[211] but computer programs have allowed this task to be automated.[212]

The accuracy of a given increment-based method is dependent on the breadth of the library it surveys. Although many increment-based methods have been found to be as good as or better than quantum chemically derived data,[68,184,212] discrepancies between experimental chemical shifts and those predicted by

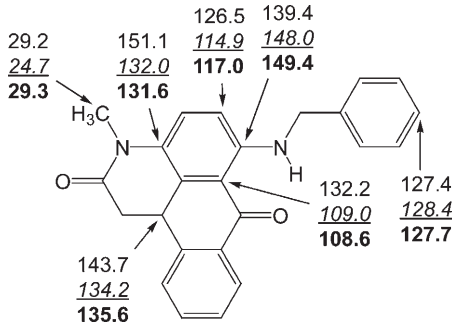

Figure 9. A dye with select ^{13}C chemical shift data (shifts that vary the most from experimental values) derived from an increment-based method (CNMR, rms error = 8.1 ppm)[213] displayed in normal text, quantum chemically derived chemical shifts (GIAO-B3LYP/MIDI!//B3LYP/MIDI!, rms error = 1.9 ppm) displayed in *underlined italics*, and experimental chemical shifts displayed in **bold**.[129]

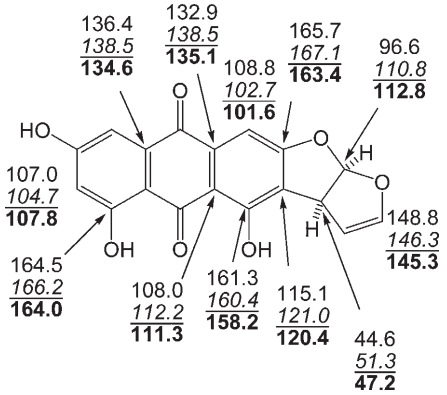

Figure 10. Versicolorin A with select ^{13}C chemical shift data (shifts that vary the most from experimental values) derived from an increment-based method [ChemNMR (implemented in ChemDraw), rms error = 3.05 ppm] displayed in normal text, quantum chemically derived chemical shifts [(GIAO)B3LYP/6-311+G(2d,p)//HF/6-31G(d), rms error = 1.86 ppm] displayed in *underlined italics*, and experimental chemical shifts displayed in **bold**.[184,214]

increment based methods often occur when the molecule of interest has nuclei with chemical shifts not well represented in the query library. It has been noted that these discrepancies can be significant; for example, in 2002 Giesen and Zumbulyadis reported a comparison of experimental ^{13}C data with both increment-based (CNMR)[213] and quantum chemically [(GIAO)-B3LYP/MIDI!//B3LYP/MIDI!] determined chemical shifts for the dye pictured in Figure 9.[129] Select chemical shifts reported by Giesen and Zumbulyadis[129] are displayed in Figure 9, and it is clear that in some cases the increment-based method predicts the chemical shift more accurately than does the quantum chemical method (e.g., shifts at 127.7 and 29.3 ppm). Note, however, that these nuclei are in environments likely to be well represented in a library of common compounds; in other cases, the increment-based method performs much more poorly than does the quantum chemical method (e.g., shifts at 131.6 and 108.6 ppm), and the overall agreement is better for the quantum chemical method.

In another example, the ^{13}C chemical shifts for versicolorin A (see Figure 10)[214] were computed using ChemNMR implemented

Table 10. Root Mean Squared Error in Predicted ^{1}H NMR Chemical Shifts[116]

method	scaled	unscaled
ChemDraw	0.311	0.329
ACD	0.176	0.185
B3LYP[a]	0.127	0.355
TPSS[a]	0.132	0.188
WP04[a]	0.135	0.226
VSXC[a]	0.154	0.215
BMK[a]	0.166	0.551

[a] CSGT with aug-cc-pVDZ basis set.

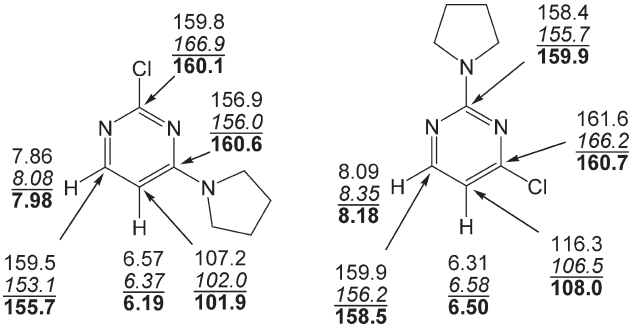

Figure 11. Two constitutional isomers of chloropyrrolidinylpyrimidine with select chemical shift data (shifts that vary the most from experimental values) derived from an increment-based method (ACD) displayed in normal text, quantum chemically derived chemical shifts [(GIAO)-B3LYP/6-31G(d,p)//B3LYP/6-31G(d,p)] displayed in *underlined italics*, and experimental chemical shifts displayed in **bold**.[39]

in ChemDraw,[36] leading to a mean average deviation nearly twice as large as that from quantum chemical calculations [3.05 vs 1.86 ppm, at the (GIAO)B3LYP/6-311+G(2d,p)//HF/6-31G(d) level of theory].[184]

In 2009, Jain, Bally and Rablen reported a comparison of increment-based (ChemDraw[36] and ACD[38]) and quantum chemical methods for the prediction of ^{1}H NMR chemical shifts for 80 small organic molecules; their results appear in Table 10.[116] This data emphasizes that increment-based methods can be useful, depending on the level of accuracy necessary to answer the questions at hand (i.e., if there is not unusual bonding, if the chemical shifts of alternative structures are not too close to those in the structure in question, etc.).

In 2006, Pérez et al. presented data obtained using several increment-based (including ACD[38] and NMRPredict[215]) and quantum chemical (including HF, B3LYP, and MP2 with various basis sets) methods.[39] It was the aim of their study to assess the performance of various methods in distinguishing between two constitutional isomers of the chloropyrrolidinylpyrimidines depicted in Figure 11. Pérez et al. discovered that the increment-based approach provided chemical shift data close enough to experimentally observed ^{13}C shifts to distinguish between the two constitutional isomers; however, this was not the case with ^{1}H data.[39] It was determined that in this case, quantum chemical computation of ^{1}H NMR properties was necessary to obtain the desired accuracy.

One significant limitation of the increment-based methods is their inability to distinguish between stereoisomers,[39] although

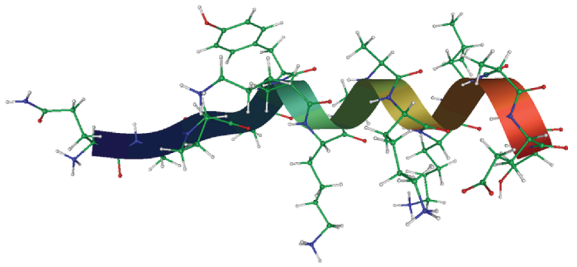

Figure 12. Crystal structure data[222] of a 15-residue fragment of human platelet factor 4 for which a (GIAO)MNDO-based method[220] was used to compute ^{1}H and ^{13}C chemical shifts.[108]

some progress is being made to this end, for example, with the universal NMR database of Kishi et al.[216−219] Kishi has synthesized several polyols, determined their ^{1}H and ^{13}C chemical shifts and coupling constants, and postulated that the stereochemistry of unknown polyols could be assigned on the basis of similarity to known polyols.[216−219] This method is based upon the principle that NMR properties are (in general) local, i.e., not significantly influenced by remote substituents. Note that this principle is also important in dealing with heavy-atom effects (section 3.5).

4.3.2. Empirically Parametrized Quantum Chemical Approaches. Although increment-based methods (section 4.3.1) may be considered to be empirically parametrized, we focus in this section on quantum chemical methods that are parametrized to reproduce experimental chemical shift data.

In 2004, Merz and co-workers described the application of a parametrized (GIAO)MNDO based semiempirical method to computation of ^{1}H and ^{13}C chemical shifts in proteins consisting of up to 107 residues.[108,220,221] One of the smaller proteins considered was a 15-residue fragment of human platelet factor 4, an experimental crystal structure of which is displayed in Figure 12 (PDB ID 1DJF).[222] Using an experimentally derived geometry (an average of 32 NMR structures), ^{1}H and ^{13}C NMR chemical shifts were computed and found to be in error by 0.30 and 2.75 ppm, respectively, on average.[108]

The speed and widespread acceptance of the B3LYP density functional has made it a target for parametrization. In 2006, Cramer et al. described the parametrization and evaluation of two new functionals—WP04 and WC04—variations of B3LYP parametrized specifically to reproduce ^{1}H and ^{13}C chemical shifts, respectively, in chloroform.[120] Table 11 summarizes the performance of various methods in computing ^{1}H and ^{13}C NMR data for a set of 43 organic molecules (160 conformers in total). From the data in Table 11 it is clear that the WC04 and WP04 functionals reproduce carbon and proton chemical shift data, respectively, with similar accuracy both with and without scaling. If scaling (see section 3.6) is applied, however, then the other density functional methods (B3LYP, PBE1, and mPW1PW91) reproduce proton data equally as well and provide a noticeable improvement for carbon data.

4.3.3. Quantum Chemical Methods. *4.3.3.1. Wave Function Theory Based Approaches.* In this section, we will consider post-Hartree−Fock-based methods for computing NMR properties of molecules. Some of these methods, which include terms for treating electron correlation, are considered "gold standards" for determining properties of molecules (NMR or otherwise).

In the most comprehensive study of this type, Gauss and Stanton used several post-HF methods to compute the isotropic shielding constants for several NMR active nuclei (^{13}C and

Table 11. Performance (mean unsigned error, ppm) of Parameterized WC04 and WP04 Density Functionals Relative to Several Other Methods[120] *a*

	unscaled		scaled	
method[a]	^{13}C	^{1}H	^{13}C	^{1}H
WC04	3.1	0.13	3.0	0.11
WP04	6.4	0.09	2.3	0.07
HF	5.8	0.17	2.8	0.12
B3LYP	6.4	0.12	2.1	0.07
PBE1	5.5	0.13	1.8	0.08
mPW1PW91	5.6	0.13	1.8	0.08

[a] GIAO method, 6-311+G(2d,p) basis set with solvent ($CHCl_3$) simulated in NMR calculation by the IEFPCM method. Geometries computed with B3LYP/6-31G(d).

Table 12. Experimentally and Computationally Determined Isotropic Shielding Constants[4,205,223]

molecule; nucleus	exptl	SCF-HF	MP2	MP3	MP4	CCSD	CCSD(T)	MCSF
CO; ^{13}C	3.29	−25.5	10.6	−4.2	12.7	0.8	5.6	8.2
CH_4; ^{13}C	198.4	194.8	201.0	198.8	199.5	198.7	199.1	198.2
CH_4; ^{1}H	–	31.7	31.4	31.5	31.5	31.5	31.5	31.3

^{1}H results appear in Table 12).[4,205,223] At first glance, the fairly large differences between computed and experimental values for ^{13}C listed in Table 12 seem somewhat disturbing, but these values are absolute isotropic shielding constants, which are much more difficult to determine accurately than are chemical shifts. Even so, all numbers appear to be converging upon the correct value with increasing computational cost (approximately left to right in Table 12). The fact that only very small molecules (CO and CH_4) were examined highlights the expense (in terms of computer time) associated with multiconfigurational calculations. Moreover, although (somewhat) larger molecules could be computed with methods such as CCSD(T), most are not, in part because of the relatively small percentage of commercial codes that incorporate this method for NMR calculations. The interested reader is directed to a report by Kupka et al.[105] that follows up on the work of Gauss and Stanton[4,205,223] by computing isotropic shielding constants for the same molecules with several DFT methods. These researchers found that in general the MP2, KT*n*, and CCSD(T) methods perform better than DFT methods and that pure DFT functionals provide more accurate shielding constants than do hybrid functionals.[105]

In 2011, Harding et al. showed that for the 1-adamantyl cation, MP2 does not suffice to reproduce ^{13}C chemical shift data; CCSD(T) provides chemical shift data with a much closer correspondence to experiment (see Table 13).[18]

In 2003, Auer, Gauss, and Stanton described the performance of some post-HF methods in comparison to two popular DFT methods for a set of 20 small molecules.[131] The standard deviations of the ^{13}C chemical shifts from those computed with CCSD(T) are displayed in Table 14. This data clearly shows that, over the 20 molecule set used, the post-HF methods MP2 and CCSD give results much closer to those of CCSD(T) than do the DFT methods (BP86 and B3LYP, unscaled). CCSD(T) is generally taken as a "gold standard," especially for geometry

dx.doi.org/10.1021/cr200106v |*Chem. Rev.* 2012, 112, 1839–1862

Table 13. MAD of ^{13}C and ^{1}H Chemical Shifts[a] for 1-Adamantyl Cation[b] Computed at Different Levels of Theory[18]

method	MAD	
	^{13}C chemical shift (ppm)	^{1}H chemical shift (ppm)
MP2/qz2p	7.95	0.19
CCSD(T)/qz2p	4.4	0.26

[a] The GIAO method was employed. [b] Geometry computed at CCSD-(T)/cc-pVTZ.

Table 14. Standard Deviation from CCSD(T) ^{13}C Chemical Shifts[131] [a]

SCF-HF	MP2	CCSD	BP86	B3LYP
10.6	2.1	1.6	6.1	7.0

[a] Methods employed qz2p basis sets and CCSD(T)/cc-pVTZ-optimized geometries.

optimization and energy determinations;[191] however, the lack of data comparing CCSD(T) and experimental ^{1}H and ^{13}C chemical shift data is a significant cause to reserve judgment.

4.3.3.2. Density Functional Theory Based Approaches. Density functional theory, due in large part to its efficiency and ease of use, has become very popular in all aspects of modern quantum chemistry, including NMR computations.[224] There have been numerous reports that describe the use of many different DFT methods in computing chemical shifts.[39,105−107,112,114,116−121,127,129,131,134,136,141,172,183,185,192,193,225−228] In this section we will present only those studies of extraordinary importance (in our opinion) or that display exceptional breadth in the methods compared.

In 2009, Jain, Bally and Rablen reported the root-mean-square error in computed ^{1}H chemical shifts for a fairly large database of 80 small organic molecules.[116] The results (Table 10) indicated that the B3LYP, TPSS, and WP04 methods, when scaled (see section 3.6), produce the least error (0.127, 0.132, and 0.135 ppm rms error, respectively).

Wu et al. provided the most extensive investigation of computed ^{13}C chemical shift data as a function of DFT functional.[107] The mean absolute deviations obtained for a 23 molecule set using a veritable alphabet soup of DFT methods appear in Table 15. Several key conclusions can be drawn from this study: (1) The MP2 (wave function based) method produces among the lowest mean absolute errors for this database. (2) The DFT methods OPBE and OPW91 produce the lowest mean absolute errors for this database. (3) The very popular DFT method B3LYP produces poor results (2.5 times the MAD of the best methods), although the computed chemical shifts were again not scaled in this study. Others have recommended the use of OPBE,[185] although in some cases B3LYP was found to be preferred to OPBE (by producing a smaller mean average deviation and less scatter in ^{13}C chemical shift data for the specific molecules examined).[119]

In 2011, Armangué et al. evaluated the efficacy of the SSB and SSB-D functionals (among others) to compute NMR shielding constants for molecules from four standard databases (WT32, HWAH8, AGS11, and HLJ5).[228] It was concluded that SSB-D and KT2 provide good results over the full range of databases (see Table 16 for data for the WT32 database). Somewhat

Table 15. MAD of Unscaled ^{13}C NMR Calculations for Various Methods over a 23 Molecule Set[107] [a]

method	MAD (ppm)	method	MAD (ppm)
HF	7.2	BLYP	5.7
MP2	2.1	BPBE	4.2
B3LYP	5.2	BPW91	4.3
O3LYP	2.4	OB98	2.9
PBE1PBE	4.4	OLYP	3.0
X3LYP	5.5	OPBE	2.0
B97-1	3.1	OPW91	2.0
B98B98	7.6	PBEB98	7.1
B98LYP	7.7	PBELYP	7.1
B98PBE	5.8	PBEPBE	5.4
B98PW91	5.9	PBEPW91	5.5
BB98	5.8		

[a] GIAO with 6-311+G(2d,p) basis set; experimentally determined geometries.

Table 16. MAD of ^{13}C and ^{1}H (GIAO) Shielding Constants[a] for the WT32 Database Computed at Different Levels of Theory[228]

method	MAD	
	^{13}C shielding constant (ppm)	^{1}H shielding constant (ppm)
PBE/ET-pVQZ	10.5	0.80
OPBE/ET-pVQZ	4.0	0.70
SSB-D/ET-pVQZ	3.6	0.70
KT2/ET-pVQZ	4.6	0.70
CCSD(T)/aug-cc-pVTZ	8.3	0.70

[a] Geometries optimized at the CCSD(T)/aug-cc-pVTZ level of theory.

remarkably, all but one of the DFT methods presented in Table 16 determines the ^{13}C shielding constant with higher accuracy (on average) than CCSD(T).

The large body of available data on applying DFT methods to chemical shift calculations is difficult to distill down, but the following conclusions seem reasonable: (1) B3LYP produces results that rival any other DFT method *if scaled*. (2) OPBE represents a reasonable alternative DFT method if one prefers not to scale computed shifts. (3) MP2 produces similar results to scaled DFT methods (although in the authors' experience MP2 quickly becomes cost prohibitive, especially when considering molecules the size of typical natural products and other synthetically relevant molecules).

4.3.3.3. Solvent Effects. Relatively few studies have concerned themselves with determining the difference between results obtained with and without solvent models or comparing results obtained using different methods for treating solvent. The most comprehensive evaluation was put forth by Jain, Bally and Rablen in 2009 (see Table 17).[116] The data in Table 17 display the average difference in chemical shift between calculations that include solvent (using PCM-SCRF to model chloroform) and those that do not. These results indicate that (1) if scaling is carried out (see section 3.6), then including solvent in the NMR calculation results in slightly less error (0.002−0.035 ppm, indicated by a positive difference), and (2) if scaling is not carried out, then including solvent actually tends to *increase* error significantly (0.021−0.139 ppm for WP04, B3LYP, TPSS, and

Table 17. Difference in Root Mean Squared Error ($RMSE_{gas}$ − $RMSE_{solvent}$) for Scaled and Unscaled Calculated ^{1}H NMR Data for Various Methods with and without Solvent Modeling (PCM-SCRF to model chloroform)[116] [a]

method	difference in scaled error (ppm)	difference in unscaled error (ppm)
WP04[b]	0.009	−0.131
B3LYP[b]	0.027	−0.139
TPSS[c]	0.026	−0.021
BLYP[b]	0.035	0.079
VSXC[c]	0.023	−0.039
BMK[c]	0.002	0.147

[a] aug-cc-pVDZ basis set. [b] GIAO. [c] CSGT.

Table 18. RMSE in ^{1}H Chemical Shift Calculations and Relative CPU Time for the (GIAO)B3LYP//B3LYP/6-31G(d) Method with Various Basis Sets[116]

basis set	unscaled	scaled	relative CPU time
6-31G(d)	0.230	0.188	1
6-31G(d,p)	0.191	0.165	1.5
cc-pVDZ	0.221	0.173	2.3
6-31++G(d,p)	0.200	0.153	2.8
6-311++G(d,p)	0.206	0.153	7.2
aug-cc-pVDZ	0.280	0.133	12.7
cc-pVTZ	0.199	0.143	44.1
aug-cc-pVTZ	0.246	0.140	311.7

VSXC; BLYP and BMK result in a decrease of error). However, solvent does not *always* increase error in unscaled cases. As described above, in 2006 Pérez et al. showed that inclusion of solvent in both the optimization and NMR protocols dramatically increased (by as much as 2-fold) correlation of computed ^{13}C and ^{1}H data to experimental numbers for two constitutional isomers of chloropyrrolidinylpyrimidine (see Figure 11).[39]

In that the performance of the many different available methods for treating solvent effects in the context of NMR calculations has not been systematically assessed, it is difficult to decide if one or more methods are best-suited for capturing solvent effects.

4.4. Basis Sets

The relatively rapid speed of NMR computations has allowed for fairly extensive studies on the effect of basis set size on computed NMR properties. In 2009, Jain, Bally and Rablen reported a thorough investigation of the effect of basis set size on ^{1}H chemical shift calculations using the B3LYP density functional method.[116] Table 18 summarizes the error and associated CPU time for several basis sets. It is clear from the data that, with or without scaling, increasing basis set size (and computational time) does not necessarily result in more accurate chemical shifts, at least with B3LYP. It has been noted in other contexts that the accuracy of DFT methods is not necessarily expected to improve with increasing basis set size,[229] but the importance of using "balanced"[230] basis sets with DFT (and other types of) calculations has been noted.[231] It has been observed independently that increasing basis set size can increase error in computed ^{13}C[112,114,172,200] and ^{1}H[112,127] chemical shifts, although the increase in error is usually only by a few tenths of a ppm for ^{13}C and a few hundredths of a ppm for ^{1}H.

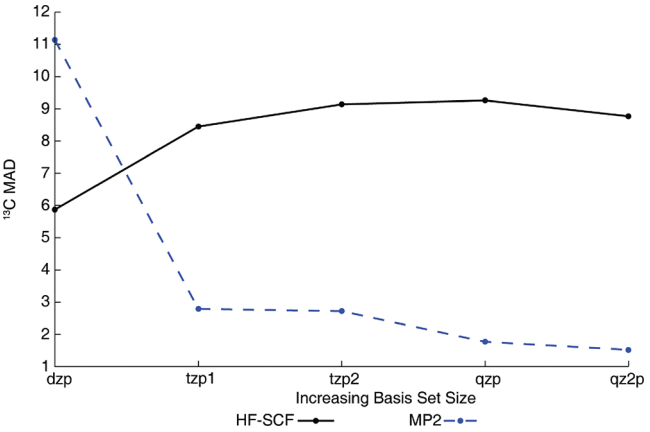

Figure 13. Mean absolute deviation of ^{13}C data as a function of basis set size for a 19 molecule set. Plot reproduced from data taken from ref 200.

Table 19. RMSE in Computed ^{13}C Isotropic Shielding Constants for Various Model Chemistries and Basis Sets[129] [a]

basis set	HF	MP2	SVWN	B3LYP	BPW91
3-21G	9.6	–	6.7	4.6	6.7
MIDI!	7.2	4.2	4.7	3.7	4.9
6-31G(d)	6.9	–	5.1	4.3	5.7
6-31+G(d)	6.2	5.3	5.2	4.2	5.7
cc-pVDZ	7.4	–	4.2	3.4	4.6
6-311+G(d)	–	–	3.0	1.9	3.2
6-311++G(d,p)	8.3	2.2	3.0	1.8	3.0

[a] Geometries at B3LYP/MIDI!.

In 1993, Gauss described the seemingly odd behavior for computed ^{13}C chemical shift data shown in Figure 13.[200] The data indicates that the error associated with increasing basis set size for the HF-SCF method appears to be parabolic in nature (i.e., error is lower for the smallest and the largest basis sets considered and higher with medium-sized basis sets). The MP2 method displays the expected behavior (increased accuracy with increasing basis set size).

If isotropic shielding constants (instead of chemical shifts) are considered, then some interesting implications come to light. In 2002, Giesen and Zumbulyadis reported the effect of basis set size on the computation of ^{13}C isotropic shielding constants (Table 19).[129] In 2008, Jensen reported a comprehensive study on ^{1}H isotropic shielding constants (see Table 20 for select data).[225] The isotropic shielding constant data presented by Giesen and Zumbulyadis (Table 19)[129] for ^{13}C and by Jensen (Table 20)[225] for ^{1}H indicate that there does exist a linear correspondence between basis set size and observed error, even for DFT methods. As described above, such a correlation was not observed for chemical shifts, so this data points to the fact that error in computed chemical shift data may be introduced by the reference standard. Scaling (see section 3.6) removes this error, at least in part. Also to this end, Sarotti and Pellegrinet suggested the use of a multireference standard (see section 5.2.2; i.e., they suggested that rather than using TMS as the reference for all carbons, one should instead use methanol for sp^3-like carbons and benzene for sp- and sp^2-like carbons), and they provided evidence that the use of such a scheme leads to a much smaller basis set dependence.[114]

Basis sets specifically designed to help reproduce NMR data, named pcJ-*n* and pcS-*n* (*n* = 0, 1, 2, etc.), also have been

dx.doi.org/10.1021/cr200106v |*Chem. Rev.* 2012, 112, 1839–1862

Table 20. MAD (ppm) of Computed ^{1}H Isotropic Shielding Constants for KT3 and B3LYP DFT Functionals and Various Basis Sets[225] [a]

	MAD		
basis set	basis functions[b]	KT3	B3LYP
STO-3G	3.9	2.4	2.4
6-31G(d,p)	11.3	0.47	0.43
cc-pVDZ	11.4	0.35	0.35
6-31++G(d,p)	14.0	0.25	0.23
aug-cc-pVDZ	18.2	0.19	0.19
6-311++G(2df,2pd)	27.1	0.10	0.11
aug-cc-pVTZ	37.3	0.10	0.11
cc-pVQZ	45.5	0.083	0.082
aug-cc-pVQZ	66.6	0.051	0.052
pcS-4	92.3	0.001	0.001

[a] Geometries taken from the G3 data set or optimized at B3LYP/6-31G(d,p) level of theory. [b] Average number of basis functions per atom.

developed.[225] These basis sets incorporate local orbitals that are "tighter" or closer to the nucleus and have been shown to lead to much lower mean average deviations for a given average number of basis functions than do Pople-,[232] Ahlrichs-,[233] or Dunning-type[234] alternatives. However, even though such basis sets are available to the community via the EMSL basis set exchange,[235−237] the fact that they are not (yet) incorporated into the most commonly available quantum chemistry codes certainly reduces their accessibility.

In 2011, Christensen et al. reported the absolute isotropic chemical shielding constants for the *cis*-*N*-amide proton of formamide.[238] In this study, basis set size was systematically varied so that extrapolation to a "complete basis set limit" could be achieved. Table 21 shows how convergence on the correct experimental value is achievable with myriad methods by extrapolating to the complete basis set limit.

5. RECOMMENDATIONS

In this section, we provide a quick reference guide to the myriad techniques, approaches, methods, problems, solutions, and recommendations presented above. Our bottom-line recommendations are based on the many reports discussed in the preceding sections, combined with our personal experience. Others, of course, may have different opinions.

5.1. Assessing Specific Sources of Error

First and foremost, researchers interested in performing chemical shift calculations must consider the nature of their system and decide which factors are important and which are not. This analysis should include determination of which specific sources of error are likely to be at play (e.g., H-bonding, section 2.2; conformational freedom, section 2.3; heavy-atom effects, section 2.5). Significant intermolecular interactions are usually relatively easy to identify, as is the potential for heavy-atom effects. The significance of conformational freedom may also initially be assessed via inspection. These quick analyses will help guide the way toward choosing the appropriate method(s) for reducing error.

5.1.1. Solvent Models. In many cases, the effect of solvent can be well-handled via a simple implicit solvent model utilized in the calculation of the absolute isotropic shielding constants. The polarizable continuum models (e.g., PCM, CPCM, SMD) coupled with UFF, UAHF, or UAKS radii have proven adequate (section 3.2). These methods are fairly simple to include in NMR single-point calculations and seem to improve results across the board. They also work well in conjunction with other techniques such as linear scaling (section 3.6). If specific intermolecular interactions are an issue, then the researcher may wish to include these explicitly in the system that is being calculated.

Table 21. Absolute Isotropic Shielding Constants (ppm) for the *cis*-*N*-Amide Proton of Formamide[238]

basis set	basis functions	CCSD(T)	CCSD	MP2	B3LYP
cc-pVDZ	57	28.06	28.09	27.90	27.67
cc-pVTZ	132	27.29	27.35	27.16	27.17
cc-pVQZ	255	26.92	27.00	26.80	26.94
cc-pV5Z	438	26.78	26.86	26.65	26.83
cc-pV∞Z	–	26.64	26.73	26.50	26.73
pcS-0	44	29.32	29.36	29.31	28.88
pcS-1	66	27.55	27.58	27.40	27.29
pcS-2	141	27.02	27.09	26.89	26.91
pcS-3	321	26.75	26.83	26.62	26.77
pcS-∞	–	26.67	26.78	26.57	26.75
experimental		26.24			

5.1.2. Conformational Averaging. If multiple conformations are likely to be accessible at experimental NMR temperatures, then these must be located either by inspection or through the use of an automated conformational search algorithm (section 3.3). In any case, once candidate conformers have been identified, their geometries and energies should be refined at an appropriate level of theory (section 5.3.1). Following this, a Boltzmann analysis should be performed in order to determine the relative contribution of each conformer and to factor in the appropriate contributions to the overall shielding constants.

5.1.3. Heavy-Atom Effects. If the molecule of interest includes heavier atoms such as sulfur or phosphorus, then methods that do a good job at handling electron correlation become even more important than usual. If the molecule contains halogen atoms and the chemical shifts of the carbon atoms directly connected to these particular nuclei are important, then extra effort is required (section 3.5). This may include the explicit account of relativistic effects via the ZORA formalism and/or a linear scaling approach based on appropriate training set data (section 3.6).

5.1.4. Rovibrational Effects. In most cases, errors due to rovibrational effects in computed chemical shifts are usually small enough to obviate extensive vibrational averaging efforts. Furthermore, general methods of error reduction (see below) serve to reduce error from this source.

5.2. General Methods of Error Reduction

Because so much of the error in computed chemical shifts is systematic in nature, we recommend using one or more methods that are adept at decreasing systematic error.

5.2.1. Linear Regression. We currently favor the linear regression approach because it allows for empirical scaling of results and provides a convenient means of converting computed shielding constants into chemical shifts without relying on any specific reference compounds (section 3.6). Furthermore, this approach has been proven applicable to numerous nuclei, including ^{1}H and ^{13}C, and thus represents a good general technique for organic molecules. The approach does require

the acquisition of a substantial amount of computational and experimental data to determine scaling factors for a given level of theory, but once this initial investment is made, scaling can be performed with minimal effort. In fact, many scaling factors have already been reported for both ^{1}H and ^{13}C for a large array of computational methods and have been shown to work well for many organic molecules (simple or complex), leading to very small average errors even with relatively affordable methods (see Appendix for discussion of our repository of scaling factors).

5.2.2. Multi-standard Approach. The multi-standard approach (section 1.2.2) produces accuracies for ^{13}C chemical shifts that rival those obtained with linear regression and thus represents a viable option for computing ^{13}C shifts when sufficient data for linear regression is not available for the particular system or computational method of interest.

5.3. Computational Methods

This section is broken down into methods for geometry optimization and for determination of the isotropic shielding constants, as the methods for these two are not inherently coupled to each other.

5.3.1. Geometry Optimization Methods. Because computed geometries turn out to be relatively consistent irrespective of the computational method used (at least for "standard" organic molecules), any one of several methods may be used here. In general, we recommend the use of B3LYP or similar density functionals, along with a basis set comparable to or larger than 6-31G(d). If relative energies are important (for example, for a Boltzmann conformational analysis), then we recommend a basis set comparable to or larger than 6-31+G(d,p).

5.3.2. Isotropic Shielding Constant Methods. Many recommendations for the choice of NMR single-point methods have been put forth in the literature. It seems as though every research group has its own preferred density functional for these calculations. Furthermore, many authors have stressed the need for large basis sets, while others have reported that smaller basis sets are perfectly adequate. In our experience, the difference between these methods diminishes significantly when linear regression is employed. However, we do find that the mPW1PW91 and PBE0 functionals provide a modest improvement over B3LYP results and that there is some benefit to using medium- to large-sized basis sets, such as 6-311+G(2d,p).

5.3.3. Our Bottom Line. All other things being equal, when we first calculate ^{1}H and ^{13}C chemical shifts for a given structure, we generally begin with an optimization at the B3LYP/6-31G(d) or B3LYP/6-31+G(d,p) level. This is then followed by an NMR single-point calculation with the B3LYP, mPW1PW91, or PBE0 functionals and a 6-311+G(2d,p) basis set, including implicit solvent modeling. We then utilize appropriate linear regression data (see the Appendix) to convert computed shielding constants into scaled computed chemical shifts. Issues with multiple accessible conformers, heavy-atom effects, and other specific sources of error are handled on a case-by-case basis.

6. CONCLUSION

The many varied reports discussed herein provide substantial evidence that highly accurate computed chemical shifts are accessible through the use of relatively affordable computational methods. Furthermore, advances in the field have provided methods of computing chemical shifts that are feasible for the nonexpert. We have compiled and presented significant evidence that such calculations can help solve many problems experienced in the day-to-day practices of synthetic organic and natural products chemistry. We hope that this review will aid the organic chemistry community in adding NMR computations to their repertoire of methods for structure elucidation.

APPENDIX: LINEAR REGRESSION SCALING FACTORS

As stated in the main body of this review, many sets of scaling factors derived from linear regression analyses have been reported. These can be quite useful to researchers who do not wish to determine such scaling factors themselves. However, reports often cover only ^{1}H or ^{13}C data, and it is not always possible to find data for both nuclei using a single computational method. This presents somewhat of a barrier for a researcher wishing to compute chemical shifts for both types of nuclei in their systems. In order to provide some improvement in this area, we have generated ^{1}H and ^{13}C scaling factors for a variety of computational methods. For the determination of these scaling factors, we have utilized the training/test set described previously by Jain, Bally and Rablen[116] for ^{1}H data, and we have adapted this training/test set for use with ^{13}C NMR computations. In addition to including the scaling factors in the Supporting Information of this review, we have created an online repository of scaling factors that can be accessed via http://cheshireNMR.info. This online repository contains our scaling factors as well as those from other contributors, and we hope that it will serve as an up-to-date source for this information now and in the future.

ASSOCIATED CONTENT

Supporting Information

^{1}H and ^{13}C scaling factors for a variety of computational methods. This material is available free of charge via the Internet at http://pubs.acs.org.

AUTHOR INFORMATION

Corresponding Author

*E-mail: tantillo@chem.ucdavis.edu.

Author Contributions

§These authors contributed equally to this report.

BIOGRAPHIES

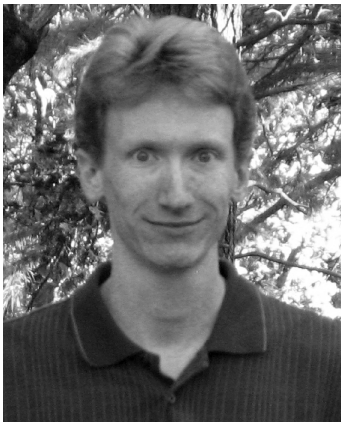

Michael Lodewyk was born in Greenbrae, California, and grew up in the greater Sacramento area. He received a B.S. degree in Chemistry in 2004 from UC Davis and a Ph.D. in 2010 from

UC Davis (under the direction of Prof. Dean Tantillo). He is currently conducting postdoctoral research with Prof. Tantillo, where he conducts mechanistic studies on a variety of synthetic, bio-organic, and natural product systems.

Matthew Siebert was raised in northern California. In 2005, he received his B.S. in Chemistry from the UC Davis, where he stayed to pursue a Ph.D. under the tutelage of Prof. Dean Tantillo. In 2009, he received his Ph.D. and moved to Texas Tech University to carry out postdoctoral research with Prof. William Hase. His research interests include electronic structure theory calculations and more recently chemical dynamics simulations of organic and organometallic systems. Further information can be found at his Web site: http://www.matthewrsiebert.net.

Dean Tantillo was born and raised in Quincy, Massachusetts. He received an A.B. degree in Chemistry in 1995 from Harvard University and a Ph.D. in 2000 from UCLA (under the direction of Prof. Kendall Houk). After receiving his Ph.D., he moved to Cornell University, where he carried out postdoctoral research with Prof. Roald Hoffmann. He joined the faculty at UC Davis in 2003, where he is now a full Professor. Research in Prof. Tantillo's group is driven by puzzling mechanistic questions in the areas of natural products biosynthesis, reactive intermediate chemistry, catalysis, organometallic chemistry, and stereoselective synthetic reactions. More information is available at his group's Web site: http://blueline.ucdavis.edu.

ACKNOWLEDGMENT

We gratefully acknowledge research support from NSF and supercomputing resources from the Pittsburgh Supercomputer Center. We also thank Prof. Paul Rablen (Swarthmore), Prof. Jochen Autschbach (Buffalo), and the members of the Tantillo research group at UC Davis for helpful discussions.

REFERENCES

(1) London, F. *J. Phys. Radium* **1937**, *8*, 397.
(2) For an account of Ramsey's work, see: Pyykkö, P. *Theor. Chem. Acc.* **2000**, *103*, 214.
(3) Hameka, H. F. *Advanced Quantum Chemistry*; Addison-Wesley: Reading, MA, 1963.
(4) Facelli, J. C. *Concepts Magn. Reson. A* **2004**, *20A*, 42.
(5) Ditchfield, R. *Mol. Phys.* **1974**, *27*, 789.
(6) Kutzelnigg, W. *Isr. J. Chem.* **1980**, *19*, 193.
(7) Schindler, M.; Kutzelnigg, W. *J. Chem. Phys.* **1982**, *76*, 1919.
(8) Schindler, M. *J. Am. Chem. Soc.* **1987**, *109*, 1020.
(9) For a comprehensive bibliography of this work, see: Schleyer, P. v. R.; Maerker, C. *Pure Appl. Chem.* **1995**, *67*, 755. See also ref 10 for a more recent review of computational NMR techniques applied to carbocations.
(10) Siehl, H.-U. *Adv. Phys. Org. Chem.* **2008**, *42*, 125.
(11) Bühl, M.; Schleyer, P. v. R. *J. Am. Chem. Soc.* **1992**, *114*, 477.
(12) For leading references to applications for boron compounds, see: Bühl, M.; Schleyer, P. v. R. In *Electron Deficient Boron and Carbon Clusters*; G. A. Olah, K. Wade, R. E. Williams, Eds.; Wiley: New York, 1991; Chapter 4.
(13) Bühl, M. In *Encyclopedia of Computational Chemistry*; Schleyer, P. v. R; Schreiner, P. R.; Allinger, N. L.; Clark, T.; Gasteiger, J.; Kollmann, P.; Schaefer, H. F., III, Eds.; Wiley: Chichester, 1998, p 1835.
(14) *Calculation of NMR and EPR Parameters*; Kaupp, M., Bühl, M., Malkin, V. G., Eds; Wiley-VCH: Verlag, 2004.
(15) Rasul, G.; Chen, J. L.; Prakash, G. K. S.; Olah, G. A. *J. Phys. Chem. A* **2010**, *114*, 4394.
(16) Wolinski, K.; Hinton, J. F.; Pulay, P. *J. Am. Chem. Soc.* **1990**, *112*, 8251.
(17) Rauhut, G.; Puyear, S.; Wolinski, K.; Pulay, P. *J. Phys. Chem.* **1996**, *100*, 6310.
(18) Harding, M. E.; Gauss, J.; Schleyer, P. v. R. *J. Phys. Chem. A.* **2011**, *115*, 2340.
(19) Alkorta, I.; Elguero, J. Computational NMR Spectroscopy. In *Computational Spectroscopy: Methods, Experiments and Applications*; Grunenberg, J., Ed.; Wiley-VCH: Weinheim, Germany, 2010; p 37.
(20) Casabianca, L. B.; de Dios, A. C. *J. Chem. Phys.* **2008**, *128*, 052201-1.
(21) Mulder, F. A. A.; Filatov, M. *Chem. Soc. Rev.* **2010**, *39*, 578.
(22) Petrovic, A. G.; Navarro-Vázquez, A.; Alonso-Gómez, J. L. *Curr. Org. Chem.* **2010**, *14*, 1612.
(23) Barone, V.; Improta, R.; Rega, N. *Acc. Chem. Res.* **2008**, *41*, 605.
(24) Bifulco, G.; Dambruoso, P.; Gomez-Paloma, L.; Riccio, R. *Chem. Rev.* **2007**, *107*, 3744.
(25) Bagno, A.; Saielli, G. *Theor. Chem. Acc.* **2007**, *117*, 603.
(26) Helgaker, T.; Jaszuński, M.; Ruud, K. *Chem. Rev.* **1999**, *99*, 293.
(27) Bally, T.; Rablen, P. R. *J. Org. Chem.* **2011**, *76*, 4818.
(28) Costa, F. L. P.; de Albuquerque, A. C. F.; dos Santos, F. M., Jr.; de Amorim, M. B. *J. Phys. Org. Chem.* **2010**, *23*, 972.
(29) Wang, B.; Dossey, A. T.; Walse, S. S.; Edison, A. S.; Merz, K. M., Jr. *J. Nat. Prod.* **2009**, *72*, 709.
(30) Yang, J.; Huang, S.-X.; Zhao, Q.-S. *J. Phys. Chem. A* **2008**, *112*, 12132.
(31) Bagno, A.; Rastrelli, F.; Saielli, G. *Chem.—Eur. J.* **2006**, *12*, 5514.
(32) Nicolaou, K. C.; Snyder, S. A. *Angew. Chem., Int. Ed.* **2005**, *44*, 1012.
(33) Weinreb, S. M. *Acc. Chem. Res.* **2003**, *36*, 59.
(34) Bagno, A. *Chem.—Eur. J.* **2007**, *7*, 1652.
(35) Duus, J. Ø.; Gotfredsen, C. H.; Bock, K. *Chem. Rev.* **2000**, *100*, 4589.
(36) *ChemOffice*; CambridgeSoft Corp., 100 CambridgePark Drive, Cambridge, MA 02140-9802.

(37) *MestReNova*, Mestrelab Research S. L., Feliciano Barrera 9B—Bajo, 15706, Santiago de Compostela, Spain.
(38) *ACD*, Advanced Chemistry Development, Inc., 110 Yonge Street, 14th Floor, Toronto, Ontario, Candada M5C 1T4
(39) Pérez, M.; Peakman, T. M.; Alex, A.; Higginson, P. D.; Mitchell, J. C.; Snowden, M. J.; Morao, I. *J. Org. Chem.* **2006**, *71*, 3103.
(40) Facelli, J. C. *J. Phys. Chem. B* **1998**, *102*, 2111.
(41) Bugaj, M.; Baran, P. A.; Bernatowicz, P.; Brożek, P.; Kamieńska-Trela, K.; Krówczyński, A.; Kamieński, B. *Magn. Reson. Chem.* **2009**, *47*, 830.
(42) Lawson, M.; Blanda, M. T.; Staggs, S. J.; Sederholm, L. N.; Easter, D. C. *J. Phys. Org. Chem.* **2009**, *22*, 1212.
(43) Karabacak, M.; Cinar, M.; Kurt, M. *Spectrochim. Acta, Part A* **2009**, *74*, 1197.
(44) Böhm, S.; Tomaščiková, J.; Imrich, J.; Danihel, I.; Kristian, P.; Koch, A.; Kleinpeter, E.; Klika, K. D. *J. Mol. Struct.: THEOCHEM* **2009**, *916*, 105.
(45) Vera, B.; Rodríguez, A. D.; Avilés, E.; Ishikawa, Y. *Eur. J. Org. Chem.* **2009**, 5327.
(46) Barczyński, P.; Dega-Szafran, D.; Katrusiak, A.; Perdoch, W.; Szafran, M. *J. Mol. Struct.* **2009**, *933*, 46.
(47) Juribašić, M.; Tušek-Božić, L. *J. Mol. Struct.* **2009**, *924—926*, 66.
(48) Kurosu, H.; Yamamoto, Y.; Fujikawa, A.; Kawabata, E.; Sone, M.; Naga, N. *J. Mol. Struct.* **2009**, *921*, 208.
(49) Saielli, G.; Nicolaou, K. C.; Ortiz, A.; Zhang, H.; Bagno, A. *J. Am. Chem. Soc.* **2011**, *133*, 6072.
(50) Smith, S. G.; Goodman, J. M. *J. Am. Chem. Soc.* **2010**, *132*, 12946.
(51) Smith, S. G.; Channon, J. A.; Paterson, I.; Goodman, J. M. *Tetrahedron* **2010**, *66*, 6437.
(52) Smith, S. G.; Goodman, J. M. *J. Org. Chem.* **2009**, *74*, 4597.
(53) Barone, G.; Gomez-Paloma, L.; Duca, D.; Silvestri, A.; Riccio, R.; Bifulco, G. *Chem.—Eur. J.* **2002**, *8*, 3233.
(54) Barone, G.; Duca, D.; Silvestri, A.; Gomez-Paloma, L.; Riccio, R.; Bifulco, G. *Chem.—Eur. J.* **2002**, *8*, 3240.
(55) Lodewyk, M. W.; Tantillo, D. J. *J. Nat. Prod.* **2011**, *74*, 1339.
(56) Schwartz, B. D.; White, L. V.; Banwell, M. G.; Willis, A. C. *J. Org. Chem.* **2011**, *76*, 8560.
(57) Lyčka, A.; Luňák, S., Jr.; Aysha, T.; Holuša, R.; Hrdina, R. *Tetrahedron Lett.* **2010**, *51*, 3149.
(58) Muñoz, M. A.; Joseph-Nathan, P. *Magn. Reson. Chem.* **2009**, *47*, 578.
(59) Umeda, R.; Fukuda, H.; Miki, K.; Rahman, S. M. A.; Sonoda, M.; Tobe, Y. *C. R. Chimie* **2009**, *12*, 378.
(60) Saielli, G.; Bagno, A. *Org. Lett.* **2009**, *11*, 1409.
(61) Williams, A. J.; Elyashberg, M. E.; Blinov, K. A.; Lankin, D. C.; Martin, G. E.; Reynolds, W. F.; Porco, J. A., Jr.; Singleton, C. A.; Su, S. *J. Nat. Prod.* **2008**, *71*, 581.
(62) Rychnovsky, S. D. *Org. Lett.* **2006**, *8*, 2895.
(63) Porco, J. A., Jr.; Su, S.; Lei, X.; Bardhan, S.; Rychnovsky, S. D. *Angew. Chem., Int. Ed.* **2006**, *45*, 5790.
(64) Hong, Y. J.; Tantillo, D. J. *Org. Lett.* **2011**, *13*, 1294.
(65) Weitman, M.; Lerman, L.; Cohen, S.; Nudelman, A.; Major, D. T.; Gottlieb, H. E. *Tetrahedron* **2010**, *66*, 1465.
(66) Micco, S. D.; Chini, M. G.; Riccio, R.; Bifulco, G. *Eur. J. Org. Chem.* **2010**, 1411.
(67) Stappen, I.; Buchbauer, G.; Robien, W.; Wolschann, P. *Magn. Reson. Chem.* **2009**, *47*, 720.
(68) Mendoza-Espinoza, J. A.; López-Vallejo, F.; Fragoso-Serrano, M.; Pereda-Miranda, R.; Cerda-García-Rojas, C. M. *J. Nat. Prod.* **2009**, *72*, 700.
(69) Hu, G.; Liu, K.; Williams, L. J. *Org. Lett.* **2008**, *10*, 5493.
(70) Timmons, C.; Wipf, P. *J. Org. Chem.* **2008**, *73*, 9168.
(71) Grube, A.; Köck, M. *Angew. Chem., Int. Ed.* **2007**, *46*, 2320.
(72) Wipf, P.; Kerekes, A. D. *J. Nat. Prod.* **2003**, *66*, 716.
(73) Dodziuk, H.; Szymanski, S.; Jazwinski, J.; Ostrowski, M.; Demissie, T. B.; Ruud, K.; Kus, P.; Hopf, H.; Lin, S.-T. *J. Phys. Chem. A* **2011**, *115*, 10638.
(74) Meiler, J.; Will, M. *J. Am. Chem. Soc.* **2002**, *124*, 1868.
(75) Elyashberg, M.; Williams, A. J.; Blinov, K. *Nat. Prod. Rep.* **2010**, *27*, 1296.
(76) Schleyer, P. v. R.; Sieber, S. *Angew. Chem., Int. Ed.* **1993**, *32*, 1606.
(77) Schleyer, P. v. R.; Laidig, K.; Wiberg, K. B.; Saunders, M.; Schindler, M. *J. Am. Chem. Soc.* **1988**, *110*, 300.
(78) Siehl, H.-U.; Vrček, V. Calculation of NMR Parameters in Carbocation Chemistry. In *Calculation of NMR and EPR Parameters*; Kaupp, M., Bühl, M., Malkin, V. G., Eds; Wiley-VCH: Verlag, 2004; pp 371.
(79) McCalum, J. E. B.; Kuniyoshi, C. Y.; Foote, C. S. *J. Am. Chem. Soc.* **2004**, *126*, 16777.
(80) Ponec, R.; Yuzhakov, G.; Tantillo, D. J. *J. Org. Chem.* **2004**, *69*, 2992.
(81) Klärner, F.-G.; Kahlert, B.; Nellesen, A.; Zienau, J.; Ochsenfeld, C.; Schrader, T. *J. Am. Chem. Soc.* **2006**, *128*, 4831.
(82) Mugridge, J. S.; Bergman, R. G.; Raymond, K. N. *J. Am. Chem. Soc.* **2011**, *133*, 11205.
(83) Gryff-Keller, A.; Szczeciński, P. *J. Mol. Struct.* **2010**, *967*, 94.
(84) Fonseca, A. C.; Jarmelo, S.; Carvalho, R. A.; Fausto, R.; Gil, M. H.; Simões, P. N. *J. Phys. Chem. B* **2010**, *114*, 6156.
(85) Yamashkin, S. A.; Alyamkina, E. A. *Chem. Hetrocycl. Compd.* **2009**, *45*, 1121.
(86) Mohamed, T. A.; Shabaam, I. A.; Zoghaib, W. M.; Husband, J.; Farag, R. S.; Alajhaz, A. E.-N. M. A. *J. Mol. Struct.* **2009**, *938*, 263.
(87) Krawczyk, H. *J. Pharm. Biomed. Anal.* **2009**, *49*, 945.
(88) Valiulin, R. A.; Dressen, D. G.; Riggs, J. R.; Habte, F. M.; Kutateladze, A. G. *J. Org. Chem.* **2009**, *74*, 3484.
(89) Dabbagh, H. A.; Rasti, E.; Grel, P. L.; Hocquet, A. *Tetrahedron* **2010**, *66*, 2322.
(90) Stewart, I. C.; Benitez, D.; O'Leary, D. J.; Tkatchouk, E.; Day, M. W.; Goddard, W. A., III; Grubbs, R. H. *J. Am. Chem. Soc.* **2009**, *131*, 1931.
(91) Justino, L. L. G.; Ramos, M. L.; Abreu, P. E.; Carvalho, R. A.; Sobral, A. J. F. N.; Scherf, U.; Burrows, H. D. *J. Phys. Chem. B.* **2009**, *113*, 11808.
(92) Zheng, F.; Dwoskin, L. P.; Crooks, P. A.; Zhan, C.-G. *Theor. Chem. Acc.* **2009**, *124*, 269.
(93) Nazarski, R. B. *J. Phys. Org. Chem.* **2009**, *22*, 834.
(94) de Oliveira, D. M.; Silva, G. D.; de, F.; Duarte, L. P.; Filho, S. A. V.; Guimarães, L.; Duarte, H. A.; de Souza, E. *Struct. Chem.* **2009**, *20*, 1005.
(95) Gonçalves, B. T.; Esteves, P. M.; Pinto, A. C.; Kaiser, C. R.; da Silva, F. L.; Miguez, E.; da Silva, J. F. M. *Magn. Reson. Chem.* **2008**, *46*, 418.
(96) Belostotskii, A. M. *J. Org. Chem.* **2008**, *73*, 5723.
(97) Poudel, P. P.; Chen, J.; Cammers, A. *Eur. J. Org. Chem.* **2008**, 5511.
(98) Gancheff, J. S.; Kremer, C.; Seoane, G.; Ventura, O. N.; Domínguez, S. *J. Mol. Struct.* **2008**, *892*, 146.
(99) Price, D. R.; Stanton, J. F. *Org. Lett.* **2002**, *4*, 2809.
(100) Nazarski, R. B.; Pasternak, B.; Leśniak, S. *Tetrahedron* **2011**, *67*, 6901.
(101) Chen, Z.; Wannere, C. S.; Corminboeuf, C.; Puchta, R.; Schleyer, P. v. R. *Chem. Rev.* **2005**, *105*, 3842.
(102) Chen, Z.; Heine, T.; Schleyer, P. v. R.; Sundholm, D. Aromaticity Indices from Magnetic Shieldings. In *Calculation of NMR and EPR Parameters*; Kaupp, M., Bühl, M., Malkin, V. G., Eds; Wiley-VCH: Verlag, 2004; p 395.
(103) Searles, D. J.; Huber, H. Molecular Dynamics and NMR Parameter Calculations. In *Calculation of NMR and EPR Parameters*; Kaupp, M., Bühl, M., Malkin, V. G., Eds; Wiley-VCH: Verlag, 2004; pp 175—190.
(104) Eriksen, J. J.; Olsen, J. M. H.; Aidas, K.; Ågren, H.; Mikkelsen, K. V.; Kongsted, J. *J. Comput. Chem.* **2011**, *32*, 2853.
(105) Kupka, T.; Stachów, M.; Nieradka, M.; Kaminsky, J.; Pluta, T. *J. Chem. Theory Comput.* **2010**, *6*, 1580.
(106) Truhlar, D. G.; Zhao, Y. *J. Phys. Chem. A.* **2008**, *112*, 6794.

(107) Wu, A.; Zhang, Y.; Xu, X.; Yan, Y. *J. Comput. Chem.* **2007**, *28*, 2431.
(108) Wang, B.; Brothers, E. N.; van der Vaart, A.; Merz, K. M., Jr. *J. Chem. Phys.* **2004**, *120*, 11392.
(109) Semiempirical methods have been employed from time to time. See refs 239 and 240.
(110) Dybiec, K.; Gryff-Keller, A. *Magn. Reson. Chem.* **2009**, *47*, 63.
(111) Baldridge, K. K.; Siegel, J. S. *J. Phys. Chem. A* **1999**, *103*, 4038.
(112) Benzi, C.; Crescenzi, O.; Pavone, M.; Barone, V. *Magn. Reson. Chem.* **2004**, *42*, S57.
(113) Schuler, R. H.; Albarran, G.; Zajicek, J.; George, M. V.; Fessenden, R. W.; Carmichael, I. *J. Phys. Chem. A* **2002**, *106*, 12178.
(114) Sarotti, A. M.; Pellegrinet, S. C. *J. Org. Chem.* **2009**, *74*, 7254.
(115) Alkorta, I.; Elguero, J. *Struct. Chem.* **2003**, *14*, 377.
(116) Jain, R. J.; Bally, T.; Rablen, P. R. *J. Org. Chem.* **2009**, *74*, 4017.
(117) Rablen, P. R.; Pearlman, S. A.; Finkbiner, J. *J. Phys. Chem. A* **1999**, *103*, 7357.
(118) Migda, W.; Rys, B. *Magn. Reson. Chem.* **2004**, *42*, 459.
(119) Aliev, A. E.; Courtier-Murias, D.; Zhou, S. *J. Mol. Struct.: THEOCHEM* **2009**, *893*, 1.
(120) Wiitala, K. W.; Hoye, T. R.; Cramer, C. J. *J. Chem. Theory Comput.* **2006**, *2*, 1085.
(121) d'Antuono, P.; Botek, E.; Champagne, B. *J. Chem. Phys.* **2006**, *125*, 144309-1.
(122) Bagno, A.; Rastrelli, F.; Saielli, G. *J. Phys. Chem. A* **2003**, *107*, 9964.
(123) Sebag, A. B.; Forsyth, D. A.; Plante, M. A. *J. Org. Chem.* **2001**, *66*, 7967.
(124) Sebag, A. B.; Friel, C. J.; Hanson, R. N.; Forsyth, D. A. *J. Org. Chem.* **2000**, *65*, 7902.
(125) Forsyth, D. A.; Sebag, A. G. *J. Am. Chem. Soc.* **1997**, *119*, 9483.
(126) Konstantinov, I.; Broadbelt, L. J. *J. Phys. Chem. A* **2011**, *115*, 12364
(127) Wang, B.; Fleischer, U.; Hinton, J. F.; Pulay, P. *J. Comput. Chem.* **2002**, *22*, 1887.
(128) Chesnut, D. B. The Ab Initio Computation of Nuclear Magnetic Resonance Chemical Shielding. In *Reviews in Computational Chemistry*; Lipkowitz, K. B., Boyd, D. B., Eds.; VCH Publishers: New York, 1996; Vol. 8, p 245.
(129) Giesen, D. J.; Zumbulyadis, N. *Phys. Chem. Chem. Phys.* **2002**, *4*, 5498.
(130) Chesnut, D. B. *Chem. Phys.* **1997**, *214*, 73.
(131) Auer, A. A.; Gauss, J. *J. Chem. Phys.* **2003**, *118*, 10407.
(132) Gauss, J.; Stanton, J. F. Electron-Correlated Methods for the Calculation of NMR Chemical Shifts. *In Calculation of NMR and EPR Parameters*; Kaupp, M., Bühl, M., Malkin, V. G., Eds; Wiley-VCH: Verlag, 2004; p 123.
(133) Gauss, J.; Stanton, J. F. *J. Mol. Struct.: THEOCHEM* **1997**, *398*−*399*, 73.
(134) Mothana, B.; Ban, F.; Boyd, R. J. *Chem. Phys. Lett.* **2005**, *401*, 7.
(135) Barić, D.; Maksić, Z. B.; Yáñez, M. *Mol. Phys.* **2003**, *101*, 1377.
(136) Wiitala, K. W.; Al-Rashid, Z. F.; Dvornikovs, V.; Hoye, T. R.; Cramer, C. J. *J. Phys. Org. Chem.* **2007**, *20*, 345.
(137) Ruden, T. A.; Ruud, K. Ro-Vibrational Corrections to NMR Parameters. In *Calculation of NMR and EPR Parameters*; Kaupp, M., Bühl, M., Malkin, V. G., Eds; Wiley-VCH: Verlag, 2004; p 153.
(138) Ruud, K.; Åstrand, P.-O.; Taylor, P. R. *J. Am. Chem. Soc.* **2001**, *123*, 4826.
(139) Autschbach, J.; Zheng, S. *Annu. Rep. NMR Spectrosc.* **2009**, *67*, 1.
(140) Neto, A. C.; Ducati, L. C.; Rittner, R.; Tormena, C. F.; Contreras, R. H.; Frenking, G. *J. Chem. Theory Comput.* **2009**, *5*, 2222.
(141) Rozhenko, A. B.; Trachevsky, V. V. *Phosphorus, Sulfur Silicon Relat. Elem.* **2009**, *184*, 1386.
(142) Autschbach, J.; Ziegler, T. Relativistic Computation of NMR Shieldings and Spin-Spin Coupling Constants. In *Encyclopedia of Nuclear Magnetic Resonance*; Grant, D. M.; Harris, R. K., Eds.; John Wiley & Sons: Chichester, 2002; Vol. 9; p 306.
(143) Kaupp, M. Interpretation of NMR Chemical Shifts. In *Calculation of NMR and EPR Parameters*; Kaupp, M., Bühl, M., Malkin, V. G., Eds; Wiley-VCH: Verlag, 2004; p 123.
(144) Branca, M.; Alezra, V.; Kouklovsky, C.; Archirel, P. *Tetrahedron* **2008**, *64*, 1743.
(145) Barone, V.; Cimino, P.; Crescenzi, O.; Pavone, M. *J. Mol. Struct.: THEOCHEM* **2007**, *811*, 323.
(146) Dračínský, M.; Bouř, P. *J. Chem. Theory Comput.* **2009**, *6*, 288.
(147) Lin, H.; Truhlar, D. G. *Theor. Chem. Acc.* **2007**, *117*, 185.
(148) Vreven, T.; Morokuma, K. In *Annual Reports in Computational Chemistry*; Spellmeyer, D. C., Ed.; Elsevier, 2006; Vol. 2, p 35.
(149) Svensson, M.; Humbel, S.; Froese, R. D. J.; Matsubara, T.; Sieber, S.; Morokuma, K. *J. Phys. Chem.* **1996**, *100*, 19357.
(150) Bagno, A.; Rastrelli, F.; Saielli, G. *J. Org. Chem.* **2007**, *72*, 7373.
(151) *Continuum Solvation Models in Chemical Physics: From Theory to Applications*; Mennucci, B., Cammi, R., Eds; John Wiley & Sons: Chichester, England, 2007.
(152) Cammi, R.; Mennucci, B.; Tomasi, J. *J. Chem. Phys.* **1999**, *110*, 7627.
(153) Ciofini, I. Use of Continuum Solvent Models in Magnetic Resonance Parameter Calculations. In *Calculation of NMR and EPR Parameters*; Kaupp, M., Bühl, M., Malkin, V. G., Eds; Wiley-VCH: Verlag, 2004; p 191.
(154) Kongsted, J.; Ruud, K. *Chem. Phys. Lett.* **2008**, *451*, 226.
(155) Yu, A.; Liu, Y.; Wang, Y. *Chem. Phys. Lett.* **2007**, *436*, 276.
(156) Król, M.; Wrona, M.; Page, C. S.; Bates, P. A. *J. Chem. Theory Comput.* **2006**, *2*, 1520.
(157) Takano, Y.; Houk, K. N. *J. Chem. Theory. Comput.* **2005**, *1*, 70.
(158) Tomasi, J.; Cammi, R.; Mennucci, B. *Int. J. Quantum Chem.* **1999**, *75*, 783.
(159) Tomasi, J.; Persico, M. *Chem. Rev.* **1994**, *94*, 2027.
(160) Tomasi, J.; Bonaccorsi, R.; Cammmi, R.; del Valle, F. J. O. *J. Mol. Struct: THEOCHEM* **1991**, *234*, 401.
(161) Christen, M.; Van Gunsteren, W. F. *J. Comput. Chem.* **2008**, *29*, 157.
(162) Foloppe, N.; Chen, I.-J. *Curr. Med. Chem.* **2009**, *16*, 3381.
(163) Lei, H.; Duan, Y. *Curr. Opin. Struct. Biol.* **2007**, *17*, 187.
(164) *Computational Biochemistry and Biophysics*; Becker, O. M., MacKerell, A. D., Jr., Roux, B., Watanable, M., Eds; Marcel Dekker: New York, 2001.
(165) Tähtinen, P.; Bagno, A.; Klika, K. D.; Pihlaja, K. *J. Am. Chem. Soc.* **2003**, *125*, 4609.
(166) Brooks, B. R.; Brooks, C. L., III; Mackerell, A. D., Jr.; Nilsson, L.; Petrella, R. J.; Rouz, B.; Won, Y.; Archontis, G.; Bartels, C.; Boresch, S.; Caflisch, A.; Caves, L.; Cui, Q.; Dinner, A. R.; Feig, M.; Fischer, S.; Gao, J.; Hodoscek, M.; Im, W.; Kuczera, K.; Lazaridis, T.; Ma, J.; Ovchinnikov, V.; Paci, E.; Pastor, R. W.; Post, C. B.; Pu, J. Z.; Schaefer, M.; Tidor, B.; Venable, R. M.; Woodcock, H. L.; Wu, X.; Yang, W.; Yourk, D. M.; Karplus, M. *J. Comput. Chem.* **2009**, *30*, 1546.
(167) Hawkins, P. C. D.; Skillman, G.; Warren, G. L.; Ellingson, B, A.; Stahl, M. T. *J. Chem. Inf. Model.* **2010**, *50*, 572.
(168) Chen, I.-J.; Foloppe, N. *J. Chem. Inf. Model.* **2010**, *50*, 822.
(169) Atilgan, C.; Aviyente, V. *Curr. Comput.-Aided Drug Des.* **2007**, *3*, 149.
(170) Sharma, A.; Reva, I.; Fausto, R. *J. Phys. Chem. A* **2008**, *112*, 5935.
(171) Saunders, M.; Houk, K. N.; Wu, Y.-D.; Still, C.; Lipton, M.; Chang, G.; Guida, W. C. *J. Am. Chem. Soc.* **1990**, *112*, 1419.
(172) Cimino, P.; Gomez-Paloma, L.; Duca, D.; Riccio, R.; Bifulco, G. *Magn. Reson. Chem.* **2004**, *42*, S26.
(173) De Gortari, I.; Portella, G.; Salvatella, X.; Bajaj, V. S.; van der Wel, P. C. A.; Yates, J. R.; Segall, M. D.; Pickard, C. J.; Payne, M. C.; Vendruscolo, M. *J. Am. Chem. Soc.* **2010**, *132*, 5993.
(174) Atieh, Z.; Allouche, A. R.; Lazariev, A.; Van Ormondt, D.; Graveron-Demilly, D.; Aubert-Frécon, M. *Chem. Phys. Lett.* **2010**, *492*, 297.
(175) Fedorov, S. N.; Radchenko, O. S.; Shubina, L. K.; Kalinovsky, A. I.; Gerasimenko, A. V.; Popov, D. Y.; Stonik, V. A. *J. Am. Chem. Soc.* **2001**, *123*, 504.

(176) Lodewyk, M. W.; Tantillo, D. J. Unpublished results.
(177) Casella, G.; Ferrante, F.; Saielli, G. *Org. Biomol. Chem.* **2010**, *8*, 2711.
(178) Malkin, V. G.; Malkina, O. L.; Salahub, D. R. *Chem. Phys. Lett.* **1996**, *261*, 335.
(179) Autschbach, J. Calculation of Heavy-Nucleus Chemical Shifts. Relativistic All-Electron Methods. In *Calculation of NMR and EPR Parameters*; Kaupp, M.; Bühl, M.; Malkin, V. G., Eds; Wiley-VCH: Verlag, 2004; pp 227.
(180) Note that this equation provides for scaling of the isotropic values, as well as the intercept, consistent with the argument put forth by Alkorta and Elguero (ref 115).
(181) The same data may also be plotted in the form of experimental chemical shifts vs computed isotropic values (i.e., the axes may be swapped). In doing so, the associated scaling equation assumes the somewhat more intuitive form: δ = slope $\times$ σ + intercept.
(182) *Spartan'10 Tutorial & User's Guide*, Appendix K, Wavefunction, Inc.: Irvine, CA.
(183) Allen, M. J.; Keal, T. W.; Tozer, D. J. *Chem. Phys. Lett.* **2003**, *380*, 70.
(184) Zhang, Y.; Wu, A.; Xu, X.; Yan, Y. *J. Phys. Chem. A* **2007**, *111*, 9431.
(185) Zhang, Y.; Wu, A.; Xu, X.; Yan, Y. *Chem. Phys. Lett.* **2006**, *421*, 383.
(186) Zhao, Y.; Truhlar, D. G. *J. Chem. Phys.* **2006**, *125*, 194101.
(187) Coriani, S.; Marchesan, D.; Gauss, J.; Hättig, C.; Helgaker, T.; Jørgensen, P. *J. Chem. Phys.* **2005**, *123*, 184107.
(188) Bak, K. L.; Gauss, J.; Jørgensen, P.; Olsen, J.; Helgaker, T.; Stanton, J. F. *J. Chem. Phys.* **2001**, *114*, 6548.
(189) Cohen, R. D.; Sherrill, C. D. *J. Chem. Phys.* **2001**, *114*, 8257.
(190) Bühl, M.; Schleyer, P. v. R. *J. Am. Chem. Soc.* **1992**, *114*, 477.
(191) Helgaker, T.; Gauss, J.; Jørgensen, P.; Olsen, J. *J. Chem. Phys.* **1997**, *106*, 6430.
(192) Dokalik, A.; Kalchhauser, H.; Mikenda, W.; Schweng, G. *Magn. Reson. Chem.* **1999**, *37*, 895.
(193) Cheeseman, J. R.; Trucks, G. W.; Keith, T. A.; Frisch, M. J. *J. Chem. Phys.* **1996**, *104*, 5497.
(194) Schwabe, T.; Grimme, S. *Acc. Chem. Res.* **2008**, *41*, 569.
(195) Zhao, Y.; Schultz, N. E.; Truhlar, D. G. *J. Chem. Theory Comput.* **2006**, *2*, 364.
(196) Zhao, Y.; Truhlar, D. G. *J. Phys. Chem. A* **2005**, *109*, 5656.
(197) Zhao, Y.; González-García, N.; Truhlar, D. G. *J. Phys. Chem. A* **2005**, *109*, 2012.
(198) Boese, A. D.; Martin, J. M. L. *J. Chem. Phys.* **2004**, *121*, 3405.
(199) For example cases where differences in connectivity/branching leads to differences in 1,3-alkyl−alkyl interactions, also known as proto-branching, see refs 241−244.
(200) Gauss, J. *J. Chem. Phys.* **1993**, *99*, 3629.
(201) Keith, T. A.; Bader, R. F. W. *Chem. Phys. Lett.* **1992**, *194*, 1.
(202) Keith, T. A.; Bader, R. F. W. *Chem. Phys. Lett.* **1993**, *210*, 223.
(203) Hansen, A. E.; Bouman, T. D. *J. Chem. Phys.* **1985**, *82*, 5035.
(204) The name "gauge-including"[203] provides the most accurate description of the method, but "gauge-invariant"[5] or "gauge-independent" are often used interchangeably. Recently, "gauge-independent" has been noted as incorrect and its use should be avoided.[19]
(205) Gauss, J.; Stanton, J. F. *Adv. Chem. Phys.* **2002**, *123*, 355.
(206) Lazzeretti, P.; Malagoli, M.; Zanasi, R. *Chem. Phys. Lett.* **1994**, *220*, 299.
(207) Steiner, E.; Fowler, P. W. *J. Phys. Chem. A* **2001**, *105*, 9553.
(208) Steiner, E.; Fowler, P. W. *Chem. Commun* **2001**, 2220.
(209) Lazzeretti, P. *Phys. Chem. Chem. Phys.* **2004**, *6*, 217.
(210) Ligabue, A.; Sauer, S. P. A.; Lazzeretti, P. *J. Chem. Phys.* **2007**, *126*, 154111.
(211) Pretsch, E.; Bühlmann, P.; Badertscher, M., *Structure Determination of Organic Compounds: Tables of Spectral Data*, 4th ed.; Springer Verlag: Berlin, 2009.
(212) Thomas, S.; Brühl, I.; Heilmann, D.; Kleinpeter, E. *J. Chem. Inf. Comput. Sci.* **1997**, *37*, 726.
(213) *CNMR*, Advanced Chemistry Development Inc., Toronto, Ontario, 2000.
(214) Gorst-Allman, C. P.; Steyn, P. S.; Wessels, P. L. *J. Chem. Soc., Perkin Trans.* **1978**, *1*, 961.
(215) *NMRPredict*. Modgraph Consultants Ltd., http://www.modgraph.co.uk
(216) Seike, H.; Ghosh, I.; Kishi, Y. *Org. Lett.* **2006**, *8*, 3861.
(217) Higashibayashi, S.; Czechtizky, W.; Kobayashi, Y.; Kishi, Y. *J. Am. Chem. Soc.* **2003**, *125*, 14379.
(218) Kobayashi, Y.; Tan, C.−H.; Kishi, Y. *Helv. Chim. Acta* **2000**, *83*, 2562.
(219) Kobayashi, Y.; Lee, J.; Tezuka, K.; Kishi, Y. *Org. Lett.* **1999**, *1*, 2177.
(220) Patchkovskii, S.; Thiel, W. *J. Comput. Chem.* **1999**, *20*, 1220.
(221) For a related example, see ref 245
(222) Montserret, R.; McLeish, M. J.; Böckmann, A.; Geourjon, C.; Penin, F. *Biochemistry* **2000**, *39*, 8362.
(223) Gauss, J.; Stanton, J. F. *J. Chem. Phys.* **1996**, *104*, 2574.
(224) It was noted that DFT is dependent on the magnetic field, calling into question whether those methods described in section 4.2 are applicable (ref 246). However, it was subsequently discovered that efforts to rigorously account for the dependence of DFT on the magnetic field resulted in data that were no more consistent with experimental NMR; see refs 107 and 247
(225) Jensen, F. *J. Chem. Theory Comput.* **2008**, *4*, 719.
(226) Magyarfalvi, G.; Pulay, P. *J. Chem. Phys.* **2003**, *119*, 1350.
(227) Koch, R.; Wiedel, B.; Wentrup, C. *J. Chem. Soc. Perkin Trans. 2* **1997**, 1851.
(228) Armangué, L.; Solà, M.; Swart, M. *J. Phys. Chem. A* **2011**, *115*, 1250.
(229) Zheng, J.; Zhao, Y.; Truhlar, D. G. *J. Chem. Theory Comput.* **2007**, *3*, 569.
(230) Formally, a balanced basis set is achieved when the number of primitive gaussians (PGs) describing the core and valence electrons for each atom is consistent.[248] For example, the 6-31G basis set for CH_3OH is considered balanced: (1) C receives six core PGs and four valence PGs, (2) O receives the same, and (3) H receives four valence PGs. Since the number of core PGs is the same for each atom (as is the number of valence PGs), this basis set is balanced. The 6-31+G(d) basis set for CH_3OH is not formally balanced (H receives four valence PGs, while C and O receive more). In practice, we find that basis sets close to balanced produce reasonable results for their computational cost.
(231) Moran, D.; Simmonett, A. C.; Leach, F. E, III; Allen, W. D.; Schleyer, P. v. R.; Schaefer, H. F., III *J. Am. Chem. Soc.* **2006**, *128*, 9342.
(232) Boys, S. F. *Proc. R. Soc. London A* **1950**, *200*, 542.
(233) Schäfer, A.; Horn, H.; Ahlrichs, R. *J. Chem. Phys.* **1992**, *97*, 2571.
(234) Dunning, T. H., Jr. *J. Chem. Phys.* **1989**, *90*, 1007.
(235) EMSL basis set exchange: https://bse.pnl.gov/bse/portal.
(236) Schuchardt, K. L.; Didler, B. T.; Elsethagen, T.; Sun, L.; Gurumoorthi, V.; Chase, J.; Li, J.; Windus, T. L. *J. Chem. Inf. Model.* **2007**, *47*, 1045.
(237) Feller, D. *J. Comput. Chem.* **1996**, *17*, 1571.
(238) Christensen, A. S.; Sauer, S. P. A.; Jensen, J. H. *J. Chem. Theory Comput.* **2011**, *7*, 2078.
(239) Heine, T.; Seifert, G. Semiempirical Methods for the Calculation of NMR Chemical Shifts. In *Calculation of NMR and EPR Parameters*; Kaupp, M., Bühl, M., Malkin, V. G., Eds; Wiley-VCH: Verlag, 2004; p 141.
(240) Hunter, C. A.; Packer, M. J.; Zonta, C. *Prog. Nucl. Magn. Reson. Spectrosc.* **2005**, *47*, 27.
(241) Fishtick, I. *J. Phys. Chem. A* **2010**, *114*, 3731.
(242) Wodrich, M. D.; Wannere, C. S.; Mo, Y.; Jarowski, P. D.; Houk, K. N.; Schleyer, P. v. R. *Chem.—Eur. J.* **2007**, *13*, 7731.
(243) Grimme, S. *Angew. Chem., Int. Ed.* **2006**, *45*, 4460.
(244) Wodrich, M. D.; Corminboeuf, C.; Schleyer, P. v. R. *Org. Lett.* **2006**, *8*, 3631.
(245) Gao, Q.; Yokojima, S.; Fedorov, D. G.; Kitaura, K.; Sakurai, M.; Nakamura, S. *J. Chem. Theory Comput.* **2010**, *6*, 1428.

(246) Koch, W.; Holthausen, M. C. In *A Chemist's Guide to Density Functional Theory*; Wiley-VCH: Verlag, Germany, 2001; p 204.
(247) Lee, A. M.; Handy, N. C.; Colwell, S. M. *J. Chem. Phys.* **1995**, *103*, 10095.
(248) Gordon, M. S.; Truhlar, D. G. *Int. J. Quantum Chem.* **1987**, *31*, 81.